ACCOUNTING FOR REMAINING INJECTED FRACTURING FLUID

A Thesis

by

YANNAN ZHANG

Submitted to the Office of Graduate and Professional Studies of
Texas A&M University
in partial fulfillment of the requirements for the degree of

MASTER OF SCIENCE

Chair of Committee,	Christine Ehlig-Economides
Committee Members,	Yuefeng Sun
	Eduardo Gildin
Head of Department,	A. Daniel Hill

December 2013

Major Subject: Petroleum Engineering

ABSTRACT

The technology of multi-stage fracturing of horizontal wells made the development of shale gas reservoirs become greatly successful during the past decades. A large amount of fracturing fluid, usually from 53,000 bbls to 81,400 bbls, is injected into the reservoir to create the fractures. However, only a small fraction of injected fracturing fluid from 10% to 40% has been recovered during the flowback process and the long term shale gas well production period. Possible mechanisms for low load recovery include ineffective dewatering of the propped fractures, matrix pore scale water retention related to imbibition, capillary fluid retention, relative permeability, and water held up in a fracture network (complexity) opened or reopened during fracture treatments.

This work is critical both to understand existing shale gas well performance and to improve shale gas well designs. Current treatment practices that promote fracture complexity as an objective may be misplaced in some shale formations. As well, the number of fractures seemingly created from so many perforation clusters per fracture stage may be undermining the ability to dewater created fractures. The insights derived from this research reveal important differences in load recovery behavior that may impact well performance in different shale formations and highlight how effectively the wells are draining the stimulated shale volume.

To my family

ACKNOWLEDGEMENTS

I would like to express my sincere gratitude to my advisor and committee chair Dr. Christine Ehlig-Economides for her dedication and support throughout my Master study and research. Also thanks to my committee members, Dr. Yuefeng Sun, Dr. Peter P. Valko and Dr.Eduardo Gildin.

Thanks to Apache Canada, Ltd., EOG Resources, Inc. and Drilling Info for providing the data for this research.

Thanks also go to my friends and colleagues and the department faculty and staff for making my time at Texas A&M University a great experience.

Finally, thanks to my mother and father, and my sister for their encouragement.

NOMENCLATURE

Y_{water}	=	Water Gas Mole Ratio, mole/mole
W	=	West
E	=	East
N	=	North
OGIP	=	Original Gas in Place, Bcf
WGR	=	water gas ratio, bbl /Mcf
T	=	Temperature, K
S	=	Water Saturation
τ	=	Scaled Time, s
φ	=	Porosity
λ	=	Gas Mobility at Mean Pressure
Π	=	Modified Pressure, $P-P_s$ atm

TABLE OF CONTENTS

LIST OF FIGURES

LIST OF TABLES

CHAPTER I

INTRODUCTION

This chapter explains the research objectives, the approach followed for the research, and the significance of the results. It ends with a summary of the thesis contents.

1.1 Study Objectives

The main objective of this work is to clarify the production mechanism of injected fracturing fluid and to characterize the impact of remaining injected fracturing fluid on the production performance of shale gas wells producing from different shale formations with different well and reservoir properties. Shale formations that appear to be adversely impacted by low load recovery could be targets for alternative treatment strategies or fracturing fluids. In particular, it may show whether to consider a different fracture fluid or whether to alter the well design.

1.2 Approach

The approach was to collect long term production data from different shale formations in the US and Canada and make diagnostic plots to analyze the flowback behavior of injected fracturing fluid. Unfortunately, most operators do not report water production data suitable for this study, and many report none at all. However, observations on shale wells in the Horn River and Barnett shale formations have revealed that the water-gas-ratio versus cumulative gas production tends to frequently exhibit 2 characteristic behavior trends. We have seen that the characteristic trend early on in production showing water-gas-ratio (WGR) to be dropping as the reciprocal square root of cumulative gas production may reflect displacement of injected fluid by produced gas. The trend for later on showing WGR dropping approximately linearly with cumulative gas production may correspond to water vaporization in the produced gas and may continue until the WGR drops to a level approximately that of water solubility in methane.

Diagnostic plots of water-gas ratio versus cumulative gas were made for 16 horizontal wells in the Horn River Shale gas reservoir and 17 horizontal wells in the Barnett Shale gas reservoir. The diagnostic plots may reveal consistent behavior for each shale but different behavior for Horn River compared to Barnett. We estimated the water solubility level for Horn River shale and Barnett shale formations and compared the WGR to this value. By this approach, we were able to see whether the long term behavior of the water-gas ratio approaches the water solubility value. Table 1.1 is a summary of all the work which has been finished.

Table 1.1: Thesis Work Plan

Thesis Work Plan(▬ Completed)	Q1-12	Q2-12	Q3-12	Q4-12	Q1-13	Q2-13	Q3-13	Q4-13
Horn River Shale Study								
Production Data Analysis	▬							
Water Entry in PL Surveys		▬						
Literature Search			▬					
Data Gathering				▬				
Water Production Analysis of Horn River Shale					▬			
Water Production Analysis of Barnett Shale						▬		
Reconciling Observations with Literature							▬	
Report Writing								▬

1.3 Significance

The observations from this work help to evaluate the shale gas well performance and to make an improvement in the shale gas well designs. Results of this research indicates differences in load recovery and well performance behavior for the Horn River and Barnett shale formations that relate to whether the wells are effectively draining the SSV.

This study helps to clarify whether low load recovery is an issue for shale gas well performance.

1.4 Thesis Summary

This thesis includes five chapters. The description of each chapter is as follows:

Chapter I: Introduction - this chapter includes the study objectives, the approach, the significance of this research work, and finally ends with the thesis summary.

Chapter II: Literature review - this chapter provides a brief review of parameters affecting fracturing fluid flow behavior in shale gas reservoirs and mechanisms impacting fracturing fluid recovery including liquid loading, water displacement and vaporization processes. A final section addresses flowback analysis and modeling.

Chapter III: Injected fracturing fluid production analysis in the Horn River Shale - this chapter analyzes the Horn River shale production data by using several diagnostic and specialized plots. The fracturing fluid flow regimes will be shown on those plots.

Then the production performance of Horn River Shale wells will be evaluated. The conclusion will be made on the kinds of water production mechanisms in Horn River Shale and the impact of load recovery on well performance.

Chapter IV: Injected fracturing fluid production behavior in the Barnett Shale – the study procedures for Barnett Shale in this chapter are the same as in Chapter III. The diagnostic and specialized plots to identify the water production regimes and potential production problems will be shown. Then the evaluation of production performance for Barnett Shale wells will be provided in this chapter. The conclusion includes the kind of water production mechanisms in Barnett Shale and the impact of load recovery on well performance.

Chapter V: Conclusions and recommendations - this chapter summarizes all the findings and results developed throughout this study and compares the similarities and differences between the Horn River Shale and Barnett Shale. This chapter analyzes the impact of load recovery on well performance of each shale. A recommendation on future work is also included.

CHAPTER II

LITERATURE REVIEW

This section provides background information about parameters affecting fracturing fluid flow behavior in shale gas reservoir, mechanisms impacting fracturing fluid recovery including liquid loading, water displacement and vaporization processes. A final section addresses flowback analysis and modeling. We begin with parameters affecting fracturing fluid flow including capillary pressure, fracture complexity, and fracture conductivity.

2.1 Capillary Pressure Effects

Mahadevan (2005)suggested that unrecovered fracturing fluid is trapped in the rock matrix near the hydraulic fracture due to the high capillary pressure in the shale matrix, and that relatively high water saturation around the hydraulic fractures reduces the relative permeability of the hydrocarbons. However, some studies showed that higher load recovery of injected fracturing fluid doesn't always result in higher gas production. Holditch (1979) indicated that if the fracturing fluid doesn't signicantly reduce the rock permeability, water will not block the gas flow, and sufficient pressure drawdown will overcome the capillary pressure and result in the same cumulative gas production. Parekh and Sharma (2004) showed that if the ratio of pressure drawdown to the capillary pressure and the relative permeability is very high, the cleanup of water block in the rock matrix will be faster.

Lolon et al. (2008) said that short-term flowbacks may cause gas phase trapping and fracture face damaging in low permeability reservoirs. Either long-term flowbacks that achieve the highest possible rate of cleanup or no “inter-stage” cleanup with rapid succession of treatment stages and commingled flowback should be considered.

2.2 Fracture Complexity Effects

King (2010) indicated that fracture complexity may be the main reason of low water load recovery. The low water load recovery may be related to relative permeability in the natural fractures, related wetting phenomena, and the tortuous path from the far reach of hydraulic fractures. The stimulated reservoir volume may be smaller than the outer extent of fracture fluid penetration. Unrecovered fracturing fluid in the smaller natural fractures may block the flow path. The capillary pressure and water saturation in the smallest pores and fractures are very high, and therefore a very high pressure drawdown is needed to start the flow. In this case gas production might be increased by reducing the capillary pressure. The backflow analysis should differentiate production performance from a fracture ranging from initial after-frac flow to stable production. In particular, capillary pressure becomes larger after the fracturing fluid is recovered at the early time and the water saturation decreases. Therefore, the volume and salinity of recovered fluids may suggest the flowback mechanisms. .

Warpinski et al. (2008) proposed that because the pressure drop and fracture network conductivity are very low, it is hard to recover water from the far reaches of the network, especially the junctions of orthogonal sets of fractures. Fast fluid cleanup and high load recovery may indicate the creation of a simple fracture instead of a significant fracture network. He also noted that the cleanup of toe stages is often not as good as the heel-side stages. Some horizontal wells are designed with a slight upward incline in order to drain water more easily.

Thompson et al. (2010) observed that higher water recovery of wells may result in lower initial production rates and higher decline. They explained load recovery of more-complex fractures is less than that of more planar-type fractures. Wells with more-complex fractures have lower fracture gradients and better production.

2.3 Effect of Fracture Conductivity

Modeland et al. (2011) said the estimated ultimate recoveries of wells are increased by less aggressively flowing them back in Haynesville shale play. The Haynesville-Bossier Shale is soft and the operator keeps a high BHFP to prevent formation fines going into the proppant pack and damaging the conductivity during the early production. The bottomhole flowing pressure declines during production, and the stress on proppant becomes larger. Because of this the propped fracture conductivity is reduced due to proppant crushing and reduced proppant porosity. Therefore higher fracture conductivity should lead to better clean-up and higher load recovery of water.

Crafton (2010) indicated that the flowback process of initially gas-filled natural fractures and gas-energized fluid systems is quite different from that of the initially liquid-filled fracture systems. The gas filled system has very high pressure and highly compressible gas “bubble” beyond the stimulation liquid and provides energy to void the hydraulic fractures. This process is not sensitive to the flowback rate. However, the liquid voidage effect of the initially liquid-filled fractures is very poor. Due to the lower compressibility and higher viscosity, a higher pressure drawdown is needed to achieve the same mass rate. The pressure gradient near the fracture face varies away from the well, particularly when fracture conductivity is low enough to result in significant pressure gradient in the fractures. Therefore, a high proppant conductivity is critical for such systems.

Crafton and Gunderson (2006) said that excessively high flowback rates can result in proppant flowback or fracture collapse. Shutting the well in before the initial production has influence on future performance.

2.4 Effect of Liquid Loading

Turner et al. (1969) said that liquid phase is produced during the natural gas production from underground reservoirs. The presence of liquid phase has an effect on the flowing characteristics of the well. The higher density liquid phase must be transported to the surface by gas. If the gas cannot provide enough energy to lift the liquid to the surface, the liquids will accumulate in the wellbore. Two physical models are proposed for the liquid removal in gas wells: liquid film movement along the walls of the pipe, and liquid droplets associated with the high velocity gas. The critical condition to transport liquids from gas wells is the high enough gas velocity to transport the largest drops to the surface.

Zhou and Yuan (2009) proposed that besides liquid film and liquid droplet mechanisms, a third mechanism liquid-droplet concentration should be considered for liquid loading in gas wells. If the liquid-droplet concentration is higher than a critical value, the critical-gas velocity changes with the concentration.

Kuru et al. (2013) suggested that non-recovered water can also accumulate in the fractures. The height of hydraulic fractures in horizontal wells is usually from tens to hundreds feet. Liquid loading in the fractures will have a great impact on the gas flow. In this case the effective stimulated shale volume would be reduced even when the pressure drawdown is greater than the capillary pressure. Two main parameters, capillary pressure and gravity, may impact the fracture drainage. Cyclic shut in and high production rates lead to proppant crushing and therefore increase the capillary pressure. The higher capillary pressure makes it difficult to clean the remaining water in the propped fractures. The direction of gravity relative to the drainage direction is related to the sweep efficiency in the fractures. Drainage in the fractures above the well is in gravity direction, and drainage in the fractures below the well is against the gravity direction. The drainage against the gravity direction is unstable and liquid loading may happen in the fractures.

Whitson et al. (2012) indicated that cyclic shut-in method can effectively prevent the liquid loading of stimulated vertical wells and horizontal multi-fractured wells in low-permeability gas reservoirs. The cyclic shut-in periods are very short, so the time required to produce ultimate economic recovery of gas will not become noticeably longer.

2.5 Impact of Water Displacement and Vaporization

These studies did not consider the vaporization of the retained water during the long term gas production.

Rushing et al. (2008) said natural gas reservoirs exploration and development activities were at depths less than 10,000 ft before 1980s. And most of these natural gas reservoirs have normal pore pressure and temperature gradients. Then natural gas reservoirs exploration and development extended to depths from 20,000 to 25,000 ft. The pore pressure and temperature gradients in many of these deep natural gas reservoirs are abnormally high. Natural gases at such high-pressure and high-temperature reservoir conditions contain a great amount of CO_2, N_2, H_2S, and water vapor. Natural gas is at thermodynamic equilibrium with the connate liquid water at first, and then will be saturated with water vapor at specific reservoir conditions. The ability of water vapor dissolved in natural gas is affected not only by reservoir pressure and temperature, but also natural gas and connate water properties. Higher reservoir temperatures and heavier hydrocarbons in natural gas can improve the water vaporization process. The amount of vaporized water will increase as the reservoir pressure decreases. Because liquid water is removed, salt concentration in the remaining connate water will increase. When salt concentration approaches the saturated conditions, mineral precipitation will happen. Salt deposition can reduce permeability in the rock pore system and cause well plugging.

Sage and Lacey (1955) conducted laboratory measurements of water vapor content under different pressures and temperatures conditions and the measurements are plotted in Figure 2.1.

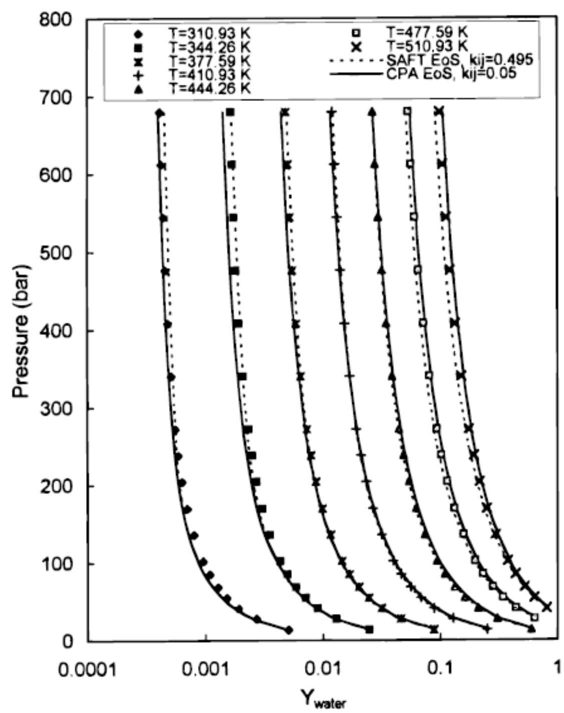

Figure 2.1: Laboratory Measurements of Water Vapor Content (Epaminondas C. Voutsas et al., 2000)

Newsham et al. (2003) conducted laboratory-based vapor desorption process and concluded that the ultra-low water saturation, abnormally high capillary pressure, and increased salinization of the water in formations may be caused by the vaporization of liquid water as gases flow through the formations.

Maxwell et al. (2008) indicated that as the gas pressure in near wellbore region is reduced, the gas becomes undersaturated. The fully saturated gas flow through the water-saturated rock and water evaporation happens. The cleanup of water blocks happens in two mechanisms. The first is immiscible displacement of water from the formation by the flowing gas. This is followed by a long time evaporation regime, often for several months. The remaining water saturation profile is different for low- or high-permeability rocks. Therefore, the resulting gas relative permeability or the well productivity depends on the rock permeability and the well drawdown. The removal of water blocks can be enhanced by: first, influencing the displacement regime; second, increasing vaporization rate by adding volatile solvents.

Maxwell et al. (2008) conducted simulations to investigate the effect of parameters such as reservoir permeability, drawdown, temperature, and the volatility of the liquid on the cleanup of water blocks.

Mahadevan et al. (2005) developed the following equation to model the evaporation regime:

$$\frac{\partial S}{\partial \tau}+\frac{A^{1/2}(\tau)}{\phi\lambda(S)}\cdot\frac{1}{\left(\frac{\Pi_0^2}{A(\tau)}-2\int_0^x\frac{1}{\lambda(S)}dx\right)^{3/2}}=0$$

Where they defined $A(\tau) = \frac{\Pi_0^2 - \Pi_L^2}{2\int_0^L \frac{1}{\lambda(S_W)} dx}$, the subscripts 0 and L corresponds to the injection and production ends. λ is the gas mobility, Π is a modified pressure, τ is scaled time, and S is the water saturation.

2.6 Flowback Analysis and Modeling

Munoz et al. (2009) suggested that segment-by-segment flowback analysis utilizing chemical tracers should be conducted to find the accurate relationship between short-term flowback and long-term post-frac performance. The initial post-frac performance is more related to the near-wellbore cleanup than the frac-tip. However, effective frac-tip cleanup can greatly improve the post-frac performance during late production.

Leonard et al. (2007) demonstrated that a higher fracturing fluid recovery may not indicate better post-completion well performance.

Willberg et al. (1998) showed a field study in the Barnett shale shows that a better fracture clean up can improve the well productivity. Both polymer and load water recovery were increased by forced closure and aggressive flowback. The Barnett shale does not produce formation water. In dry formations, such as the Barnett shale, aggressive flowback procedures can enhance fracture cleanup.

Batohie and Maharaj (2012) indicated that an area of two-phase fluid saturation is in the shale reservoir around the hydraulic fracture. The capillary pressure can hold the water in place and greatly reduce well productivity. The gas flow rate decreases due to water saturation. When the initial water saturation in a shale reservoir is below the critical water saturation (the saturation at which water begins to flow), water does not have an impact on the hydrocarbon phase flow. The capillary force is higher in tighter rock. The capillary forces in a low-permeability shale are so high that water in the near-fracture area can be imbibed into the rest of the reservoir. Then the flow barrier caused by fracturing fluid can be removed in the near-fracture reservoir area. This also allows a reduced pressure drawdown and a longer period of time that production is above the dew point and with a maximized well productivity. The effect of water bonding to clay is another mechanism of water dissipation process.

Cheng (2010) suggested that rapid imbibition of water into the matrix and dissipation of water beyond the near-fracture areas improve fracture clean up and increase gas production rate. Extended shut-in can reduce water rate and increase initial gas rate without impact on the long-term production. .

Clarkson (2012) proposed that early fluid production and flowing pressure data collected after fracture-stimulation can be used to generate long-term production forcast in shale gas reservoirs. He used the short-term flowback data to determine induced hydraulic fracture properties. The forecasts generated by flowback data fit the on-line production data very well.

Ilk et al. (2010) suggested that a log-log plot of gas water ratio versus cumulative gas can represent flow regimes of water production. But he didn't indicate what the flow regimes might indicate about the well.

2.7 Non-flowback Related Produced Water

Agnia et al. (2012) indicated that well interference has great impact on the production of hydraulically fractured horizontal shale gas wells. The gas rates decreased and water rate increased due to this reason.

Ehlig-Economides et al. (2012) also observed that some wells in Horn River shale have a large increase of water production which might come from wells in an adjacent pad during the hydraulic fracturing treatment.

2.8 Chapter Summary

This chapter has provided a literature review of previous research work about parameters affecting fracturing fluid and fracturing fluid production mechanisms. Chapter III will apply these theories and approaches to identify the fracturing fluid flow regimes in Horn River Shale and the production performance of Horn River Shale wells will be evaluated.

CHAPTER III

INJECTED FRACTURING FLUID PRODUCTION ANALYSIS IN THE HORN RIVER SHALE

Chapter II briefly described key factor impacting the fracturing fluid flow in shale gas reservoirs, possibilities may resulting in low fracturing fluid recovery, and fracturing fluid production mechanisms. This chapter will use the log-log diagnostic plot to identify the water production mechanism and potential production problems of the Horn River shale. The impact of load recovery on well performance will be investigated. We start with a general description of the shale.

3.1 Horn River Shale Reservoir Background

The Horn River Basin is in the northeastern part of British Columbia. The shale gas reservoir area is about 3 million acres on the North of Fort Nelson town, as shown in Figure 3.1. The gas shales in Horn River Basin are from the Middle and Upper Devonian periods and include the Evie, Otter Park, and Muskwa members of the Horn River Formation (Figure 3.2). The Evie and Muskwa members are the mainly developing shale gas plays because of high silica and organic contents. A 150 ft thick Middle Devonian Carbonate is between the Evie and Otter Park members as shown in Figure 3.3(Reynolds and Munn 2010).

Figure 3.1: Horn River Basin Location Map (British Columbia Ministry of Energy and Mines 2011)

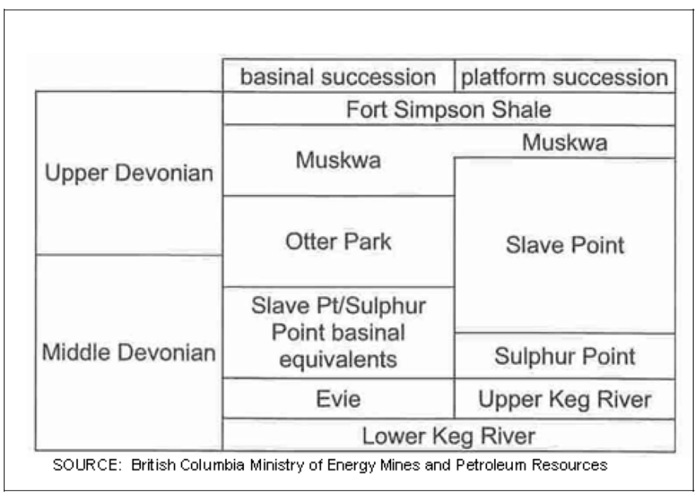

Figure 3.2: Stratigraphic Chart of the Horn River Basin (Reynolds and Munn 2010)

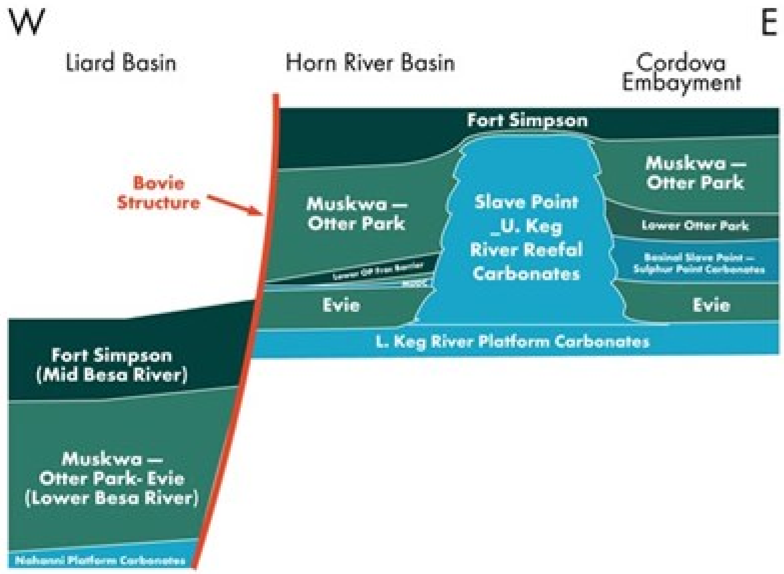

Figure 3.3: Cross-section of the Horn River Basin (Johnson et al. 2011)

The northwest heart of the Horn River Shale play is 450 to 500 ft thick, and becomes 150 ft thick and shallower in the southeast near the Peace River arch. The average depth of the Muskwa is nearly 8,500 ft TVD. The northwest deeper section is a High Pressure / High Temperature area, with a reservoir temperature of 347 °F and reservoir pressure of 7,250 psi. Some properties of the shale are listed in Table 3.1(Johnson et al. 2011).

Table 3.1: Reservoir Properties of the Horn River Basin

Properties	Value
Thickness, ft	450
Water Saturation, %	25
Matrix Permeability, nD	300
Porosity, %	3.5
Adsorbed Gas Content, %	20
Total Organic Carbon, %	3
Thermal Maturity	2.5
Silica Content, %	62
Pore Pressure Gradient, psi/ft	0.75
Raw OGIP, bcf/sec	175

The core tests show that open natural fractures exist across the basin and mini fracture tests indicate the pressure dependent leakoff. The high tectonic stress from the Rocky Mountains to the southwest area results in elevated fracture gradient. Clay content in Evie and Muskwa Shales is very low, which means the rock is brittle and suitable for hydraulic fracturing (Johnson et al. 2011).

3.2 Horn River Shale Reservoir Data Overview

This study includes analysis of 15 hydraulically fractured horizontal wells drilled from a pad in two opposing directions as shown in Figure 3.4. Wells on the northwest side of the pad was drilled across the faults mapped in Figure 3.4. Each stage has 1 – 3 perforation clusters (Ehlig-Economides et al. 2012).

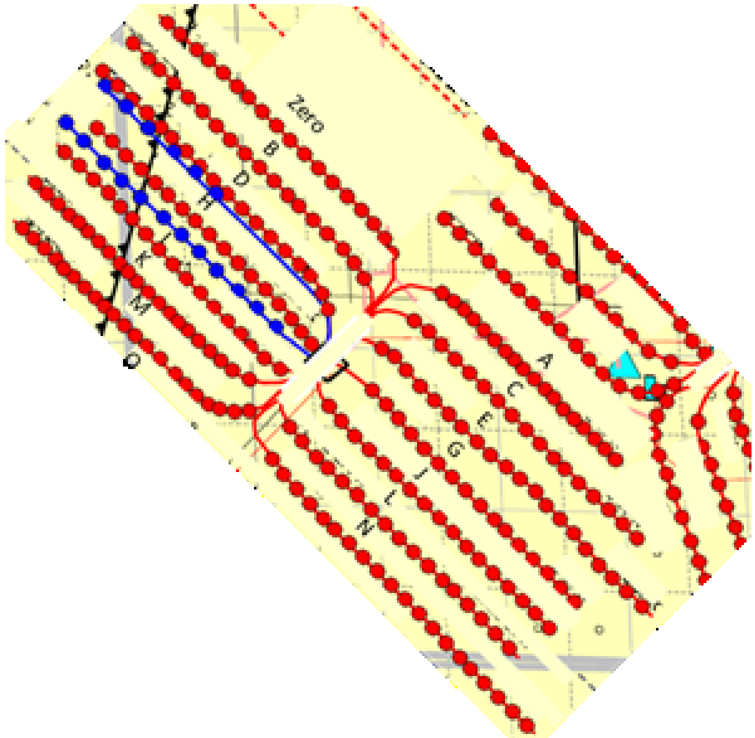

Figure 3.4: Horn River Pad Map

Production data includes daily gas and water production rate, and surface pressure during 1.8 years production period. Figure 3.5 shows the production and pressure history of one well in Horn River Shale.

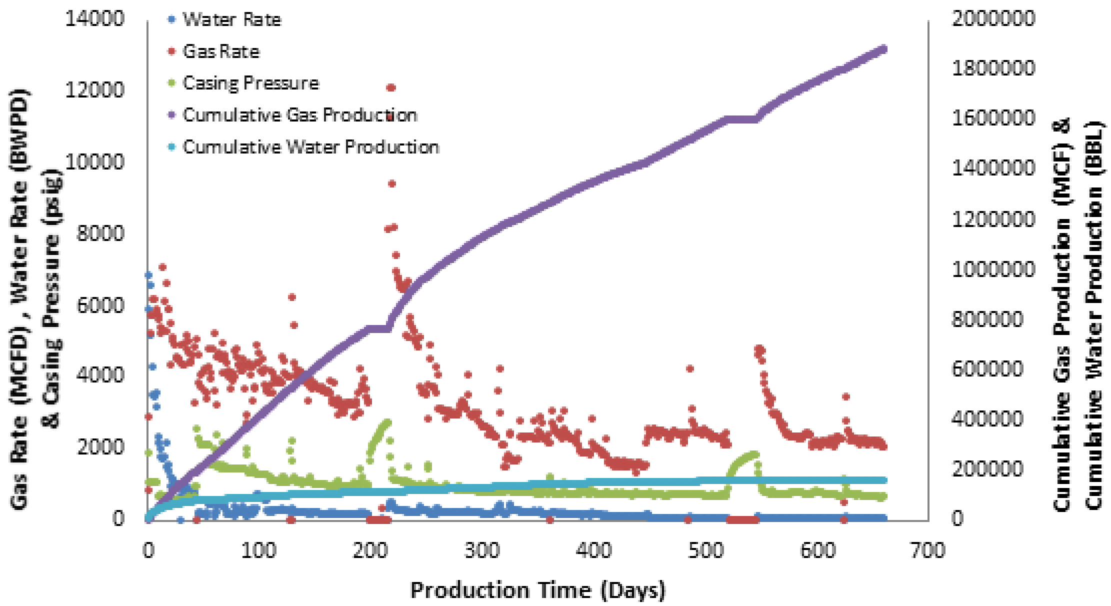

Figure 3.5: Production and Pressure History of Well in Horn River Shale

Generally water is still produced after 1.8 years of producing natural gas. The cumulative water does not level off during this time period. There are two shut-in periods can be recognized. After each shut-in period, both the gas production rates and the water production rates seem increased dramatically.

3.3 Water Production Mechanisms

In this section we provide the interpretation and analysis of gas and water production data. The production data analysis is aimed to provide indications of fracturing fluid flow regimes as well as a diagnosis of any potential production problems. The approach used in this section is that of diagnostic plots and specialized plots for multiple-well sets of long-term production data. As suggested by one of the many suggested plots by Ilk, et al. (2010), the log-log graph of water-gas-ratio (WGR) versus cumulative gas production shows a characteristic trend for the Horn River wells.

In Figure 3.6 we provide a combined plot of the WGR versus cumulative gas production for all of the wells in the Horn River Shale Reservoir. This combined plot

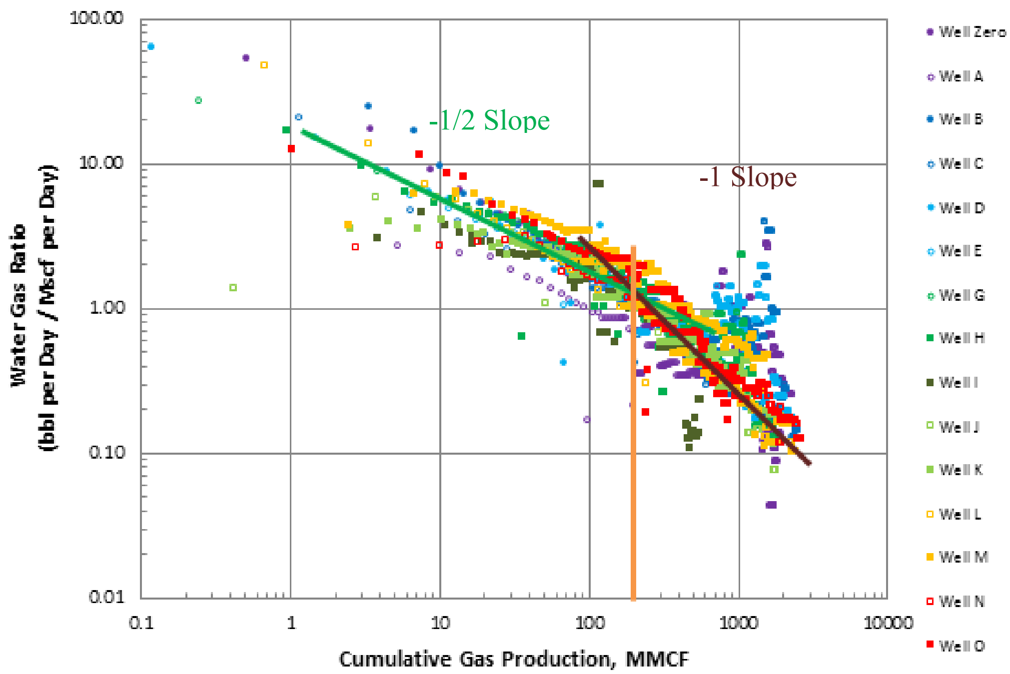

Figure 3.6: Water Gas Ratio versus Cumulative Gas Production Diagnostic Plot

shows the similarity flow trend for most of these wells. As shown in Figure 3.6, all of the analyzed 15 hydraulically fractured horizontal wells have an apparent early flow regime, which is shown as a minus half slope on the log-log plot of WGR versus cumulative gas production. Eight of the wells show in later flow regime a minus unit slope. The intersection point of minus half slope and minus unit slope is at about 200 million cubic feet.

Figure 3.7 is a Cartesian plot of water gas ratio versus cumulative gas production for all of the analyzed wells. The water gas ratio drops quickly at first and then becomes leveling off during the long term production time. Some wells have a relative higher water gas ratio compared to the other wells.

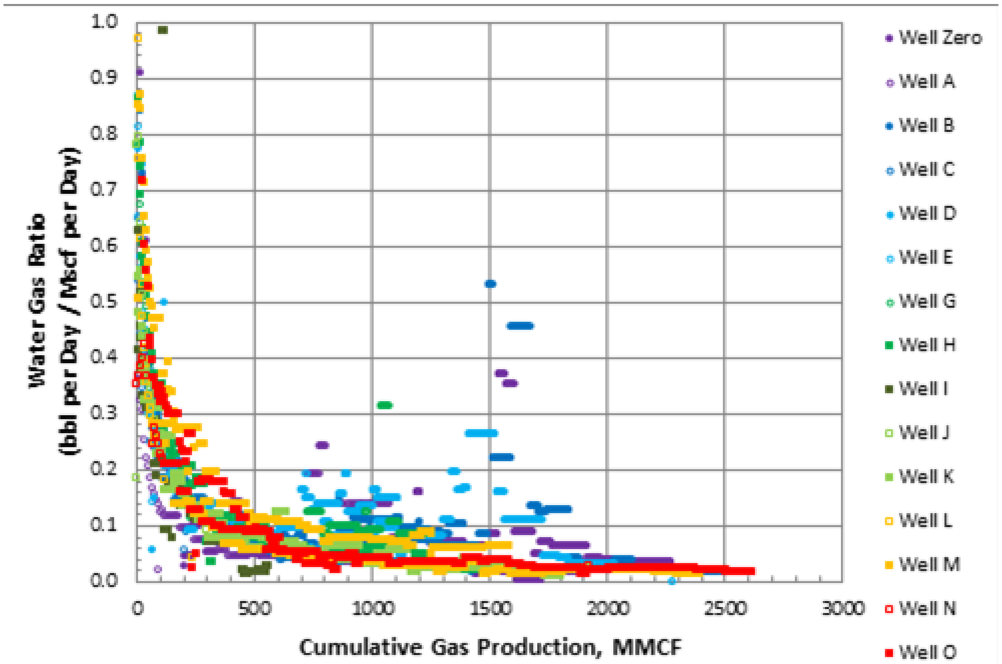

Figure 3.7: Water Gas Ratio versus Cumulative Gas Plot

Figure 3.8 is a log-log diagnostic plot of water gas ratio versus cumulative gas plot for wells with higher water gas ratio. It is clear that those wells show a minus half slope initially and then a minus unit slope for a certain time. However, those wells do not show an exactly minus unit slope because of the relative higher water gas ratio we noticed.

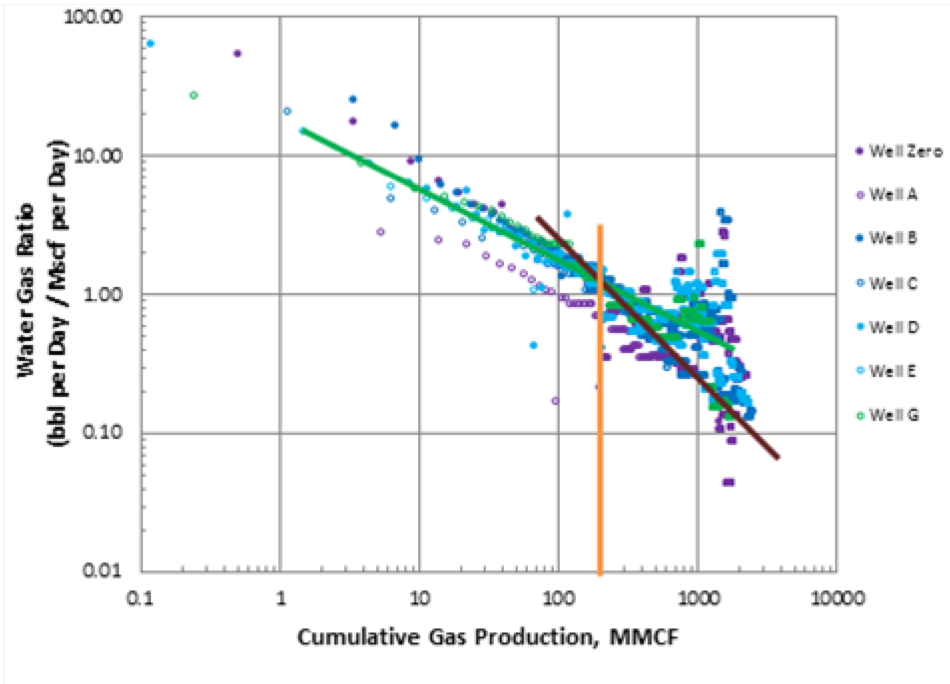

Figure 3.8: WGR vs. Cumulative Gas for Higher Water Gas Ratio Wells

Figure 3.9 is a plot of water gas ratio versus calendar time for the wells not showing the exactly late minus unite slope. It is obviously that those wells have a short period of higher water gas ratio compared to the long-term water gas ratio. The water gas ratio of those seven wells almost increased at the same time December 2010, and started to decrease in June 2011. The increased water gas ratio might be a result of drilling and completion operations in a nearby well pad.

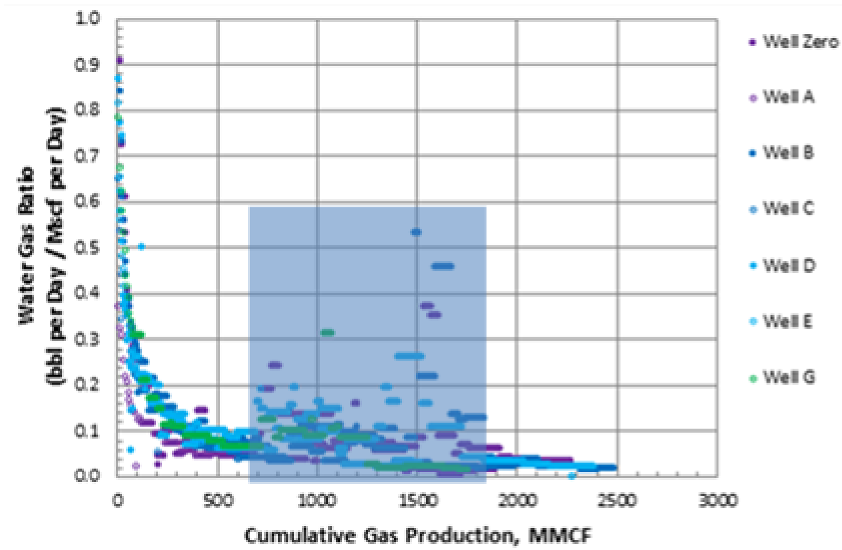

Figure 3.9: Increased Water Gas Ratio during Long-term Gas Production Period

Figure 3.10 is a Horn River pad map showing the location of the analyzed 15 horizontal wells. From this map, we noticed that all of the seven wells with increased

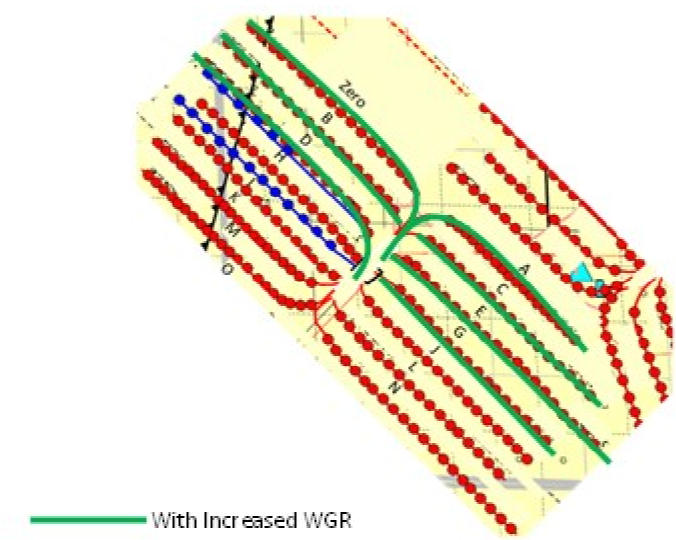

Figure 3.10: Horn River Pad Map Showing Wells With Increased WGR

water gas ratio are on the side near to a well pad under development during the time increased water production was observed in the well pad under study.

Figure 3.11 shows the timing of hydraulic fracturing operations in Horn River pad. The hydraulic fracturing stimulation of the nearby well pad began in January 2011, which is one month after the time when water gas ratio increased in Figure 3.9.

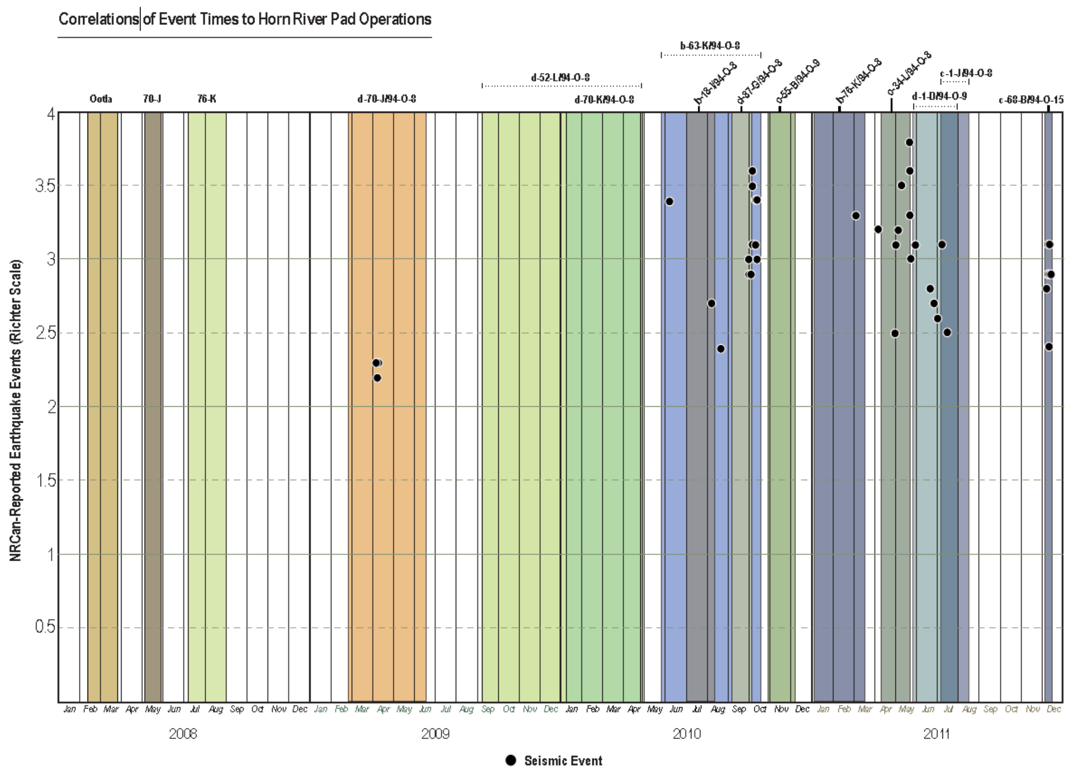

Figure 3.11: Horn River Pad Hydraulic Fracturing Operations Colored Columns (BC Oil and Gas Commission 2012)

Based on the previous observations, we made the conclusion that the increased water gas ratio in those wells cannot be caused by producing water from hydraulic fracturing operations in nearby well pad. Because of lacking drilling data from the nearby well pad, the reason of increasing water gas ratio cannot be determined.

Figure 3.12 is the log-log diagnostic plot of water gas ratio versus cumulative gas production for well O. It is obvious that well O shows a minus half slope trend during the early production time, but it does not show a minus unit slope for the long term production.

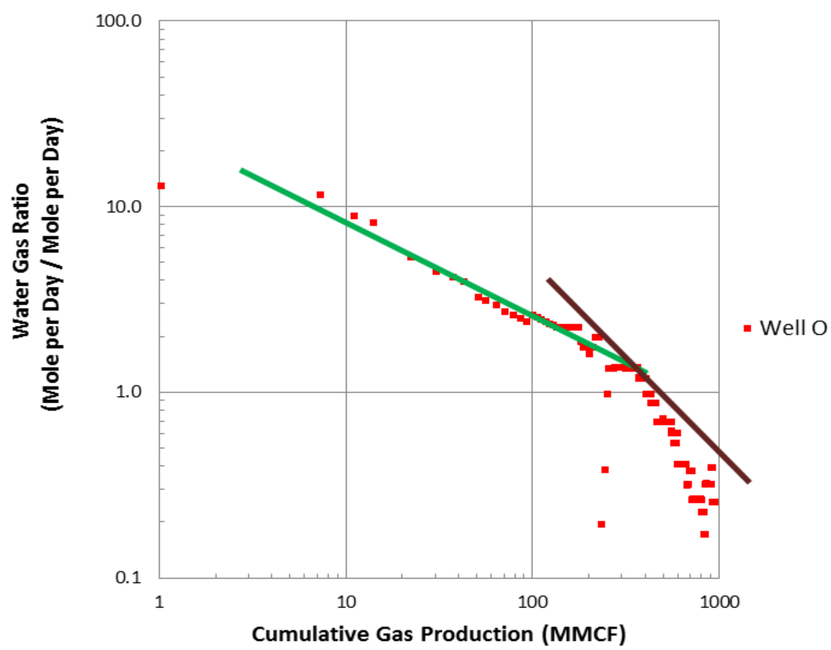

Figure 3.12: WGR vs Cumulative Gas Diagnostic Plot for Well O

Figure 3.13 shows the gas rate and water rate changing with time for well O from (Apiwathanasorn 2013). The green points in this figure indicate liquid loading in the wellbore when gas velocity is too low to lift liquid to surface. The liquid loading behavior is identified by a critical rate proposed by Turner et al. (1969). The reason that well O does not show a minus unit slope in Figure 3.12 is because of liquid loading in the wellbore.

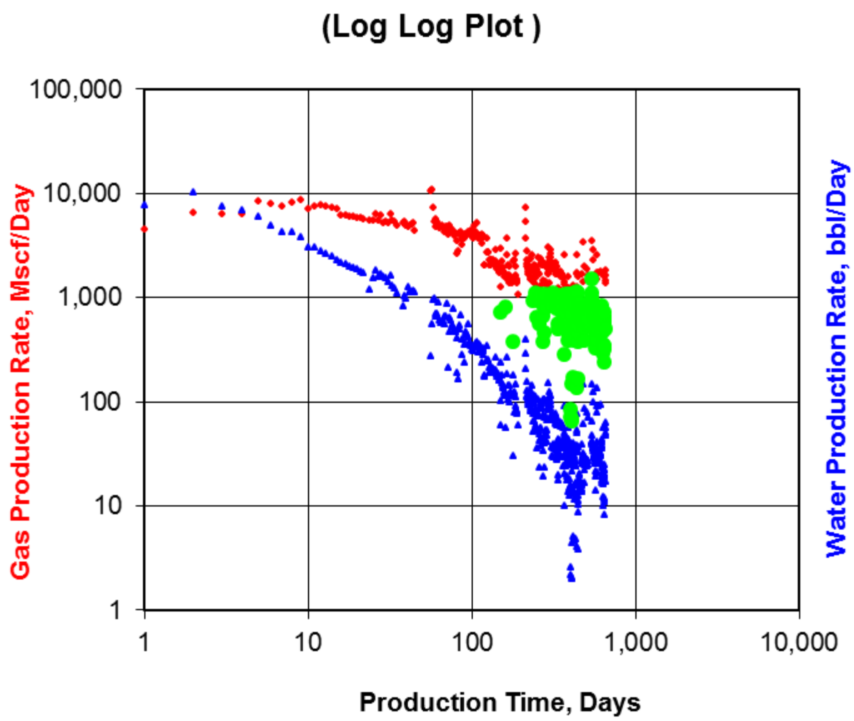

Figure 3.13: Gas Rate and Water Rate of Well O (Apiwathanasorn 2013)

As shown in the Figure 3.4, the trajectory of well O encountered the fault on the northwest side of the pad. Figure 3.14 shows the microseismic event of one stage for well O. The yellow dot is the perforation cluster. The early fracture growth started at perforation cluster and followed by a 45° change from the initial direction. Maxwell et al. (2008) explained this phenomenon happens when a propagating fracture intersects a fault.

The mapped fault is shown as a dashed line in Figure 3.14 from Ahmed and Ehlig-Economides (2013). The microseismic events with an angle to the initial fracture growth propagate along the fault. Initially the fracture opens in the direction of minimum stress. The pre-existing fault may result in the stress regime change and therefore the fracture propagation change. It is possible that liquid loading in Well O is related to intersection of the hydraulic fracture with the fault.

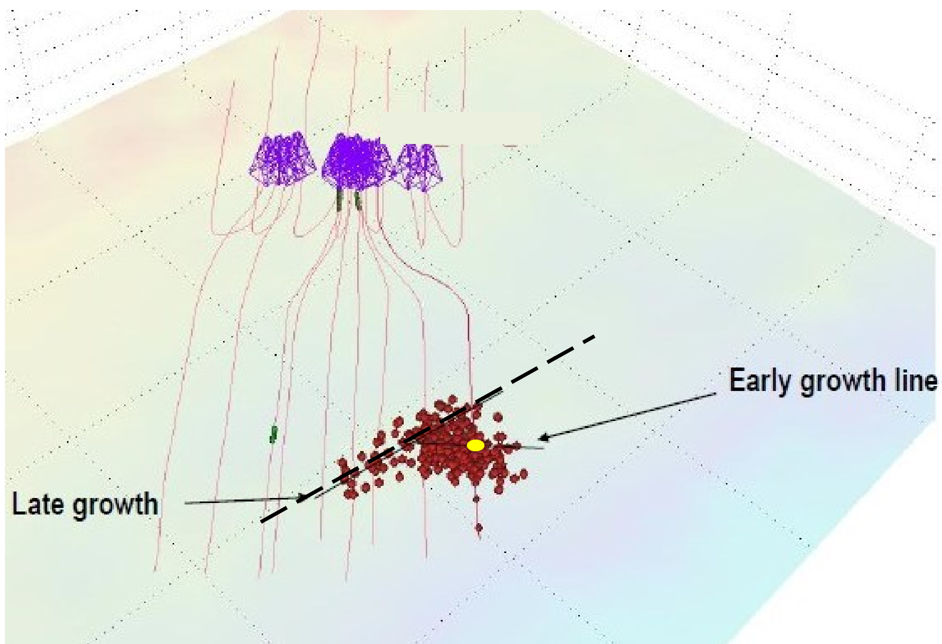

Figure 3.14: Microseismic Indicating Fracture Propagation (Ahmed and Ehlig-Economides 2013)

Water production from other source has a great impact on the accuracy of fracturing fluid production mechanism analysis. We selected wells without biased data and make the log-log diagnostic plot Figure 3.15. As shown in this figure, the water gas ratio and cumulative gas production are statistical related. The early trend on this plot is nearly minus half slope. The slope of the following trend is approach to minus one. The vertical lines mark the end of the -1/2 slope trend and the start of the approximate -1 slope trend. Figure 3.16 is a Cartesian plot of water gas ratio versus cumulative gas production, and the same trend as in Figure 3.15 is shown in this plot.

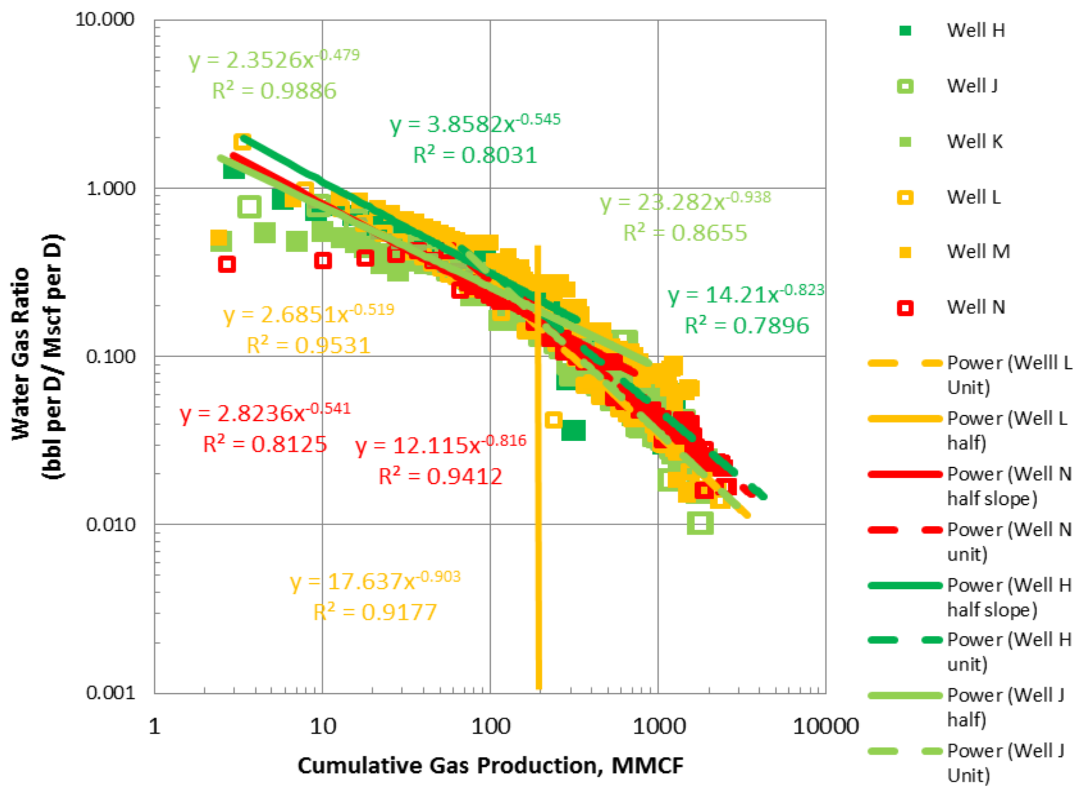

Figure 3.15: Diagnostic Plot for Wells without Abnormal Water Production

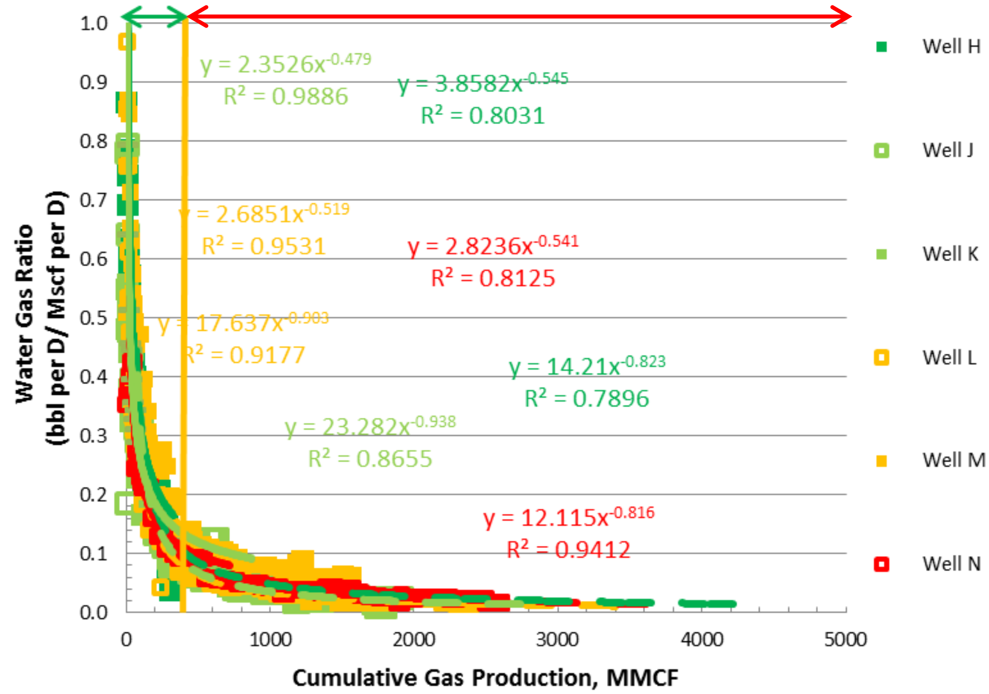

Figure 3.16: Specialized Plot Showing the Long-Term Flow Regime

We observed that the water gas mole ratio drops dramatically during the first two months of production. And then the long term water gas mole ratio becomes relatively constant for about one and half years. Mahadevan's experimental research suggested that the water-block cleanup happens in two mechanisms. The first mechanism is the immiscible displacement of the water by the flowing gas. After that, the water cleanup regime is evaporation of water by flowing gas that becomes undersaturated as the pressure decreases. The evaporation regime often lasted for a long time, sometimes on the order of months.

The reservoir pressure range in Horn River shale gas reservoir is from 313 to 471 bar. And the bottom hole flowing pressures in wells are from 45 to 70 bar. The reservoir temperature is 448 K. We used the reservoir pressures and temperature to estimate the water solubility level in Horn River shale gas reservoir as shown in Figure 3.17. The estimated water solubility level in Horn River shale gas reservoir is from 0.04-0.4.

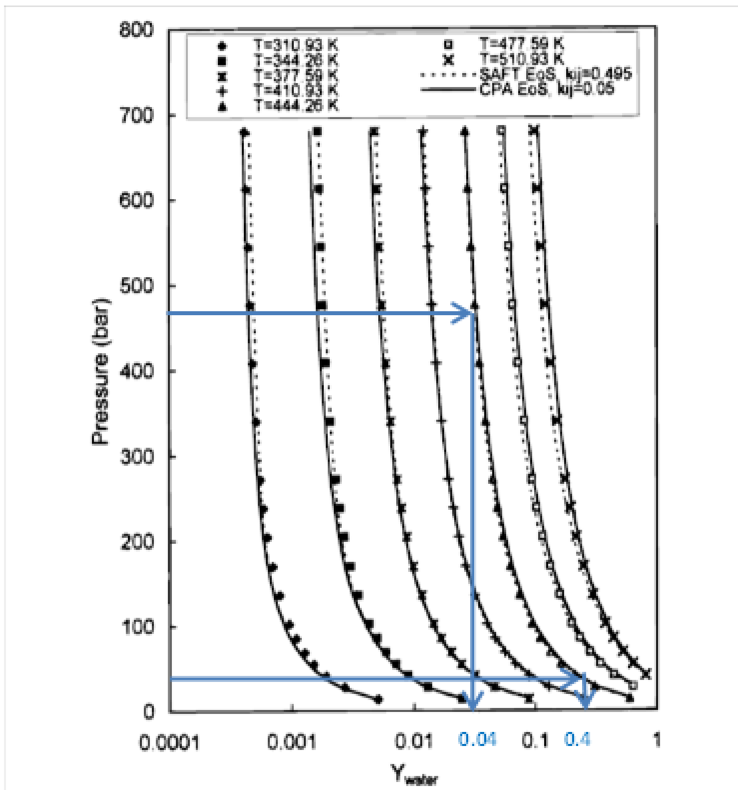

Figure 3.17: Estimated Water Solubility Level in Horn River Shale Reservoir

As shown in Figure 3.18a, the long term water gas ratio of wells in Horn River reaches the water solubility level while showing -1 slope behavior on the log-log plot, suggesting that this trend is consistent with vaporization. From Figure 3.18b, we observe that the initial steep drop in the water gas ratio represents the water displacement mechanism, corresponding to the early minus half slope in the log-log plot of water gas ratio versus cumulative gas production. The long-term relatively constant water gas ratio represents the vaporization regime, which corresponds to the later minus unit slope on the log-log diagnostic plot. The water production mechanisms in Horn River Shale are displacement of water followed by vaporization.

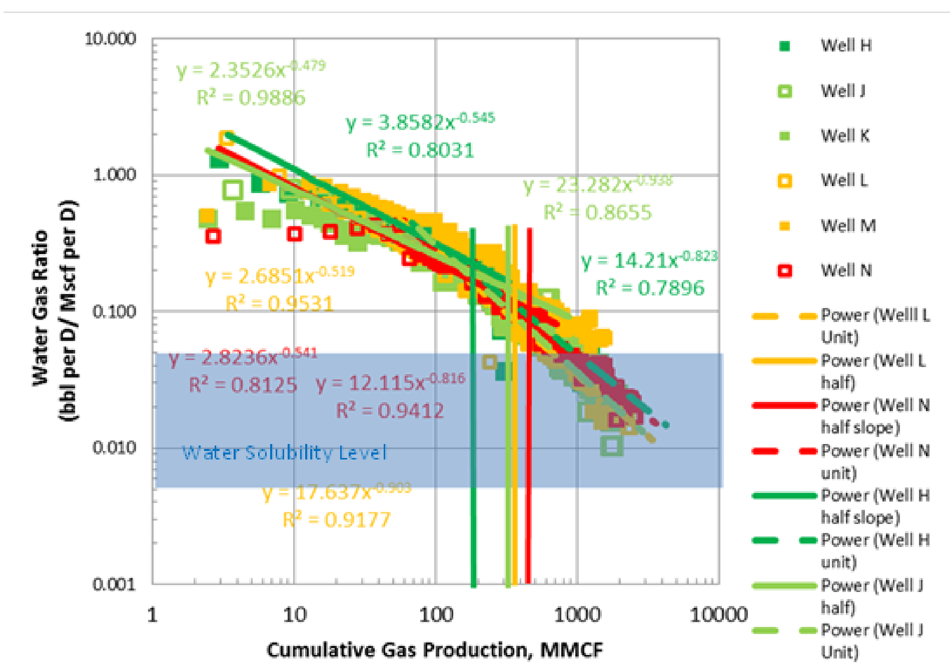

Figure 3.18 a: Log-log Plot of Water Gas Ratio versus Cumulative Gas

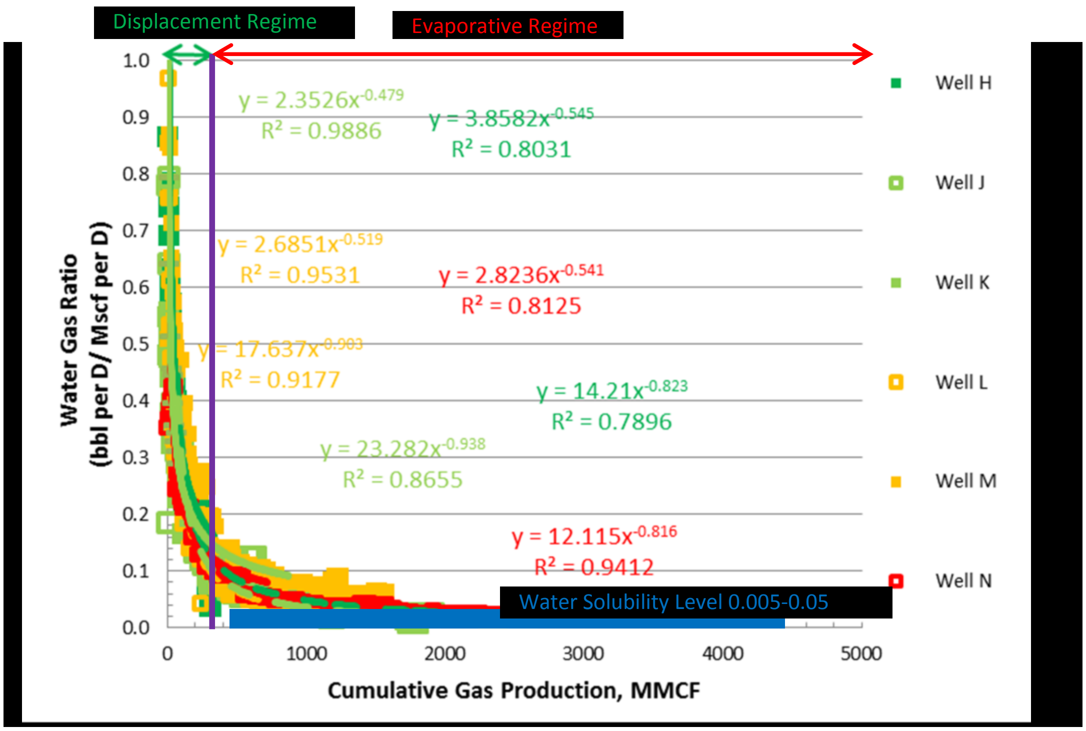

Figure 3.18b: Cartesian Plot of Water Gas Ratio versus Cumulative Gas

3.4 Analysis and Discussion of Well Performance

In this section, gas and water production rate, gas and water cumulative production, and load recovery of injected fracturing fluid will be investigated to find out whether the injected fracturing load recovery has an impact on the well production performance. The production data of 16 hydraulically fractured horizontal wells in Horn River Shale will be analyzed. As shown in Figure 3.4, the 16 horizontal wells were drilled from a pad in two opposing directions. On the northwest side of the well pad, 8 wells were drilled across the fault in Figure 3.4.

Figure 3.19 and Figure 3.20 show the cumulative water production as a function of time of wells encountered the fault and wells on the pad side without fault. As shown in these two figures well Zero, well A, well B, well C, well D, well E and well G have abnormally high cumulative water production compared to the other wells. This is because produced water not only includes injected fracturing fluid, but also water from other source as discussed in section 3.3. In Figure 3.19 we note that cumulative water production of well O grew up very quickly at first, but four months after the initial production it dropped to a very low production rate as the well became liquid-loaded. The production formation of well I is Evie, which is located below the production formation of the other wells and has the lowest cumulative water production.

The cumulative gas production as a function of time for wells on the side encountered the fault and the other side without fault is shown in Figure 3.21 and 3.22. After the first shut-in the cumulative gas production increased with the same trend as that before the shut-in. The cumulative gas production of wells encountering the mapped fault is lower than that of wells on the pad side without fault.

Those wells with abnormally high water production have the very similar cumulative gas production trend compared to other wells. The increased water production in those wells does not influence the gas production performance.

Well O has the lowest cumulative gas production because it produces from another formation Evie.

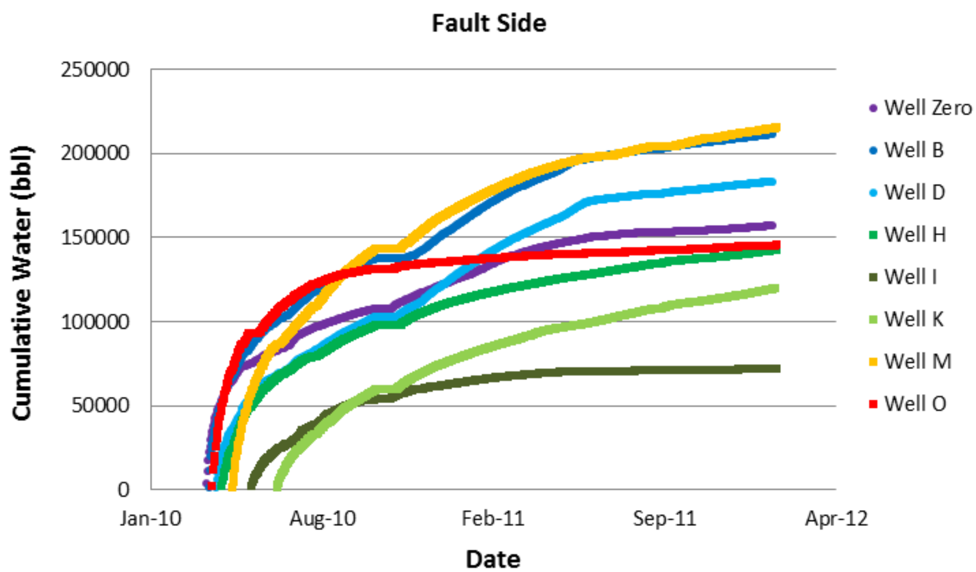

Figure 3.19: Cumulative Water Production of Wells Encountered the Fault

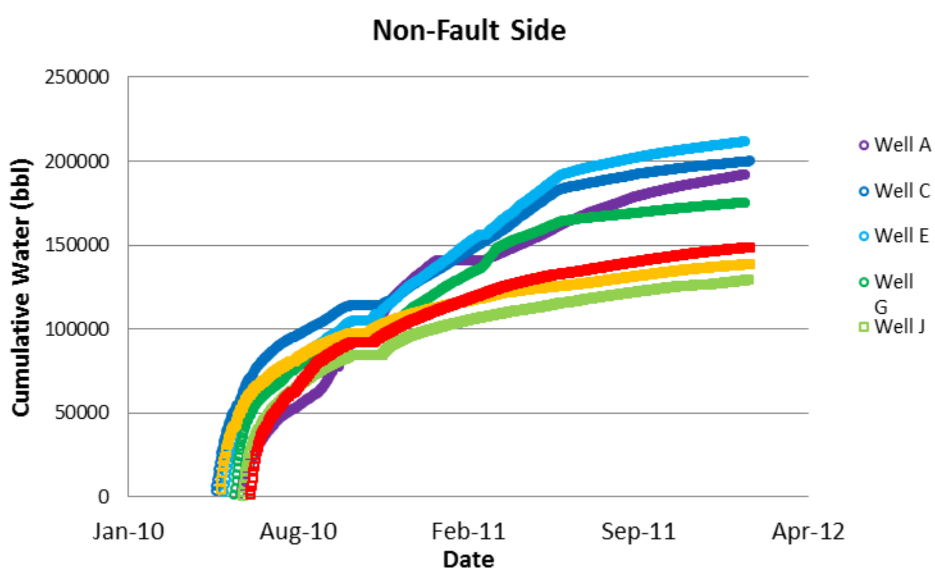

Figure 3.20: Cumulative Water Production of Wells on the Side without Fault

As shown in Figure 3.21 the cumulative gas production of well O increased with the same trend as that of the other wells initially, however, after four months' production the cumulative gas increased much more slowly. The same phenomenon is observed for well O in the Figure 3.19 of cumulative water production versus time. As being discussed in section 3.3, the microseismic events of fracture stage in well O indicate the fracture propagation is along the mapped fault, and liquid loading phenomenon is also observed in well O. The fault may has an negative impact on the production performance of well O and the resulted low gas production rates caused liquid loading phenomenon in the bottom hole of wellbore.

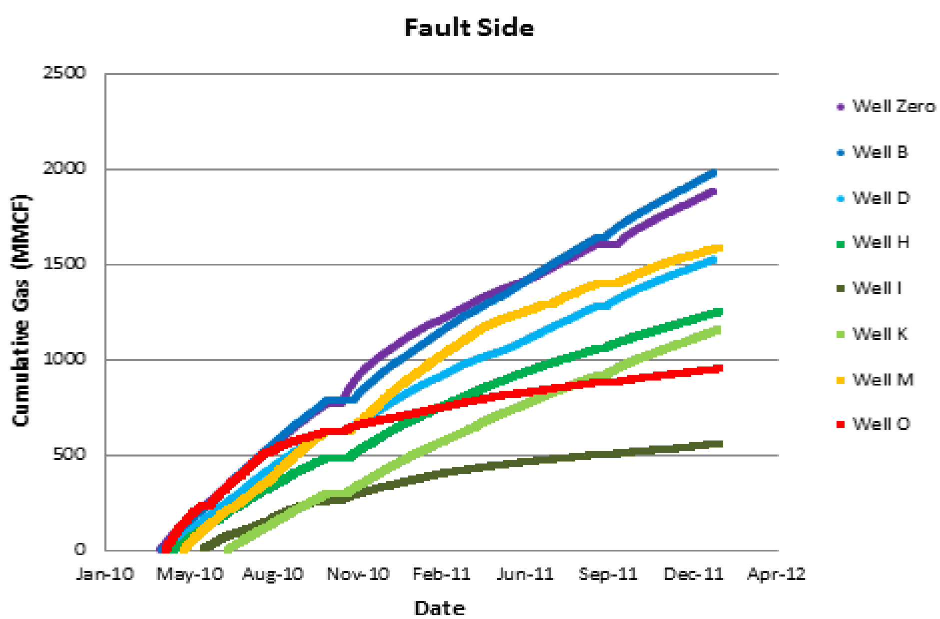

Figure 3.21: Cumulative Gas Production of Wells on the Side with the Fault

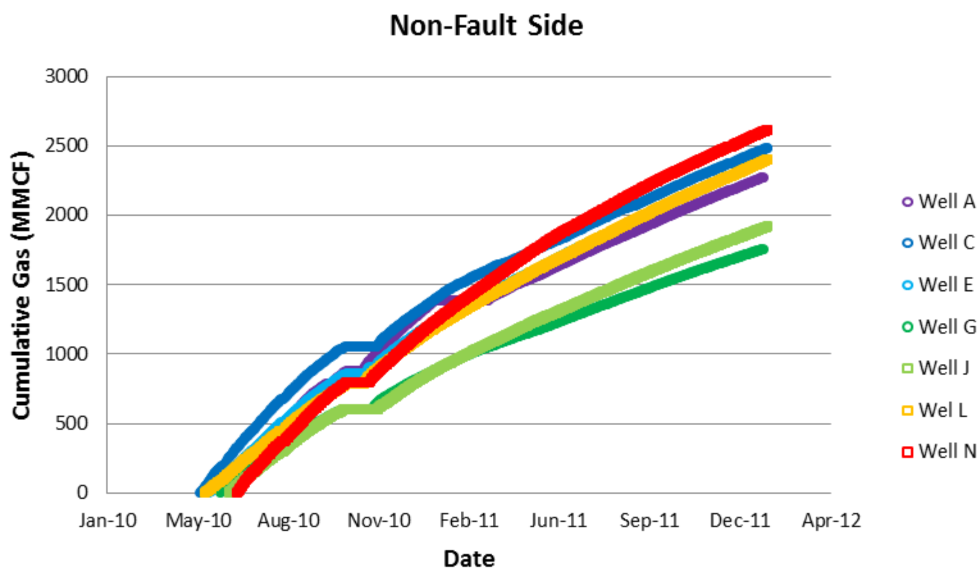

Figure 3.22: Cumulative Gas Production of Wells on the Side without the Fault

The injected fracturing fluid trapped in reservoir formations may have an impact on the well production performance. To investigate the retained water's effect on natural gas production, we tried to find the relationship between load recovery and gas production. Load recovery is the percent of recovered fracturing fluid during well production over the total amount of fracturing fluid injected into the well. Logically, water produced during drainage should impact well performance more than water produced by vaporization. Figure 3.23 is a plot of cumulative gas production versus load recovery for all of the analyzed wells. There is no clear relationship between cumulative gas and load recovery on this plot. The load recovery of wells producing water from another source may not be accurate and therefore impact the analysis result.

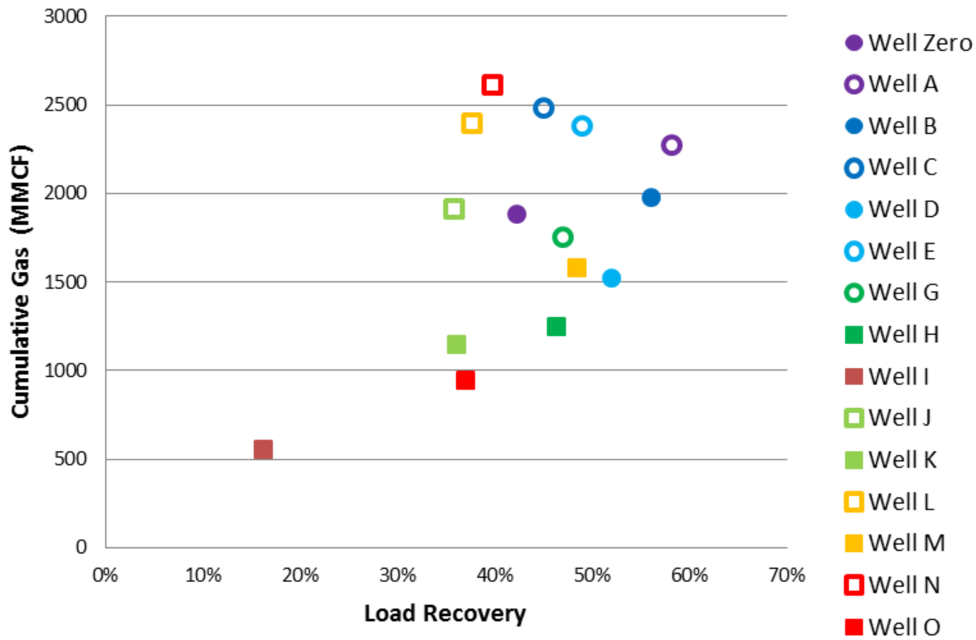

Figure 3.23: Cumulative Gas Production versus Load Recovery for All of the Wells

We selected wells without biased data and made another cumulative gas versus load recovery plot as shown in Figure 3.24. There is a very clear trend shown on this plot. The cumulative gas production increases with load recovery of fracturing fluid for wells on the pad side without a fault and also wells encountered the mapped fault. The cumulative natural gas production of wells far from the mapped fault is higher than the cumulative gas production of wells drilled across the mapped fault. The fault seems to have a negative impact on the well performance. Production logs also show that the fracture stages near to the fault do not have a good performance as those fracture stages far from the fault.

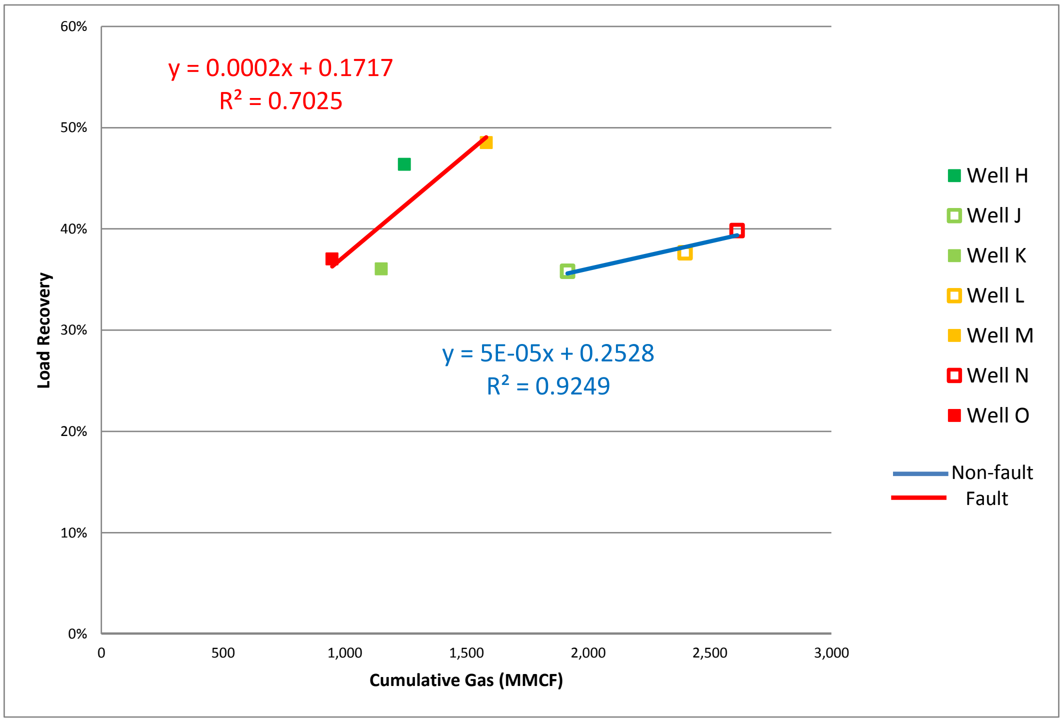

Figure 3.24: Load Recovery vs. Cumulative Gas for Wells without the Biased Data

3.5 Chapter Summary

This chapter reviewed geology background of the Horn River shale and used the log-log diagnostic plots to determine fluid flow regimes and production problems. Then analyzed well production performance.

The very high water production in several wells may come from nearby well pad during stimulation operations. The mapped fault may be connecting one of the wells with an aquifer that caused excess water production and liquid loading in the well. Cumulative gas production increased with load recovery in Horn River wells. Possibly this is because the drainage water production regime has completed in Horn River shale, and the remaining behavior is vaporization. Logically, water produced during drainage should impact well performance more than water produced by vaporization.

CHAPTER IV

INJECTED FRACTURING FLUID PRODUCTION BEHAVIOR IN THE BARNETT SHALE

This chapter will use diagnostic plots to identify water production mechanisms for the Barnett shale. As in the previous chapter, we start with geology background of the shale formation. Then the chapter will make production analysis in an analogous way to the previous chapter, but emphasizing differences in the water production behavior of the two shale formations.

4.1 Barnett Shale Reservoir Background

The Barnett Shale is located in the north-central Texas near the Muenster Arch and Ouachita Thrust Belt, and is considered as hydrocarbon source rock from middle-late Mississippian age (Figure 4.1). The depocenter of the Barnett Shale is in the northeast part of the Fort Worth basin, where the Forestburg Ls. divides the Barnett Shale into upper and lower members. The Barnett shale can be divided into 4 reservoir units (Figure 4.2). The base part of Lower Barnett Shale is Reservoir Unit 1 with the highest gamma ray. Above the Reservoir Unit 1 is Reservoir Unit 2- a carbonate zone with a medium-high gammar ray (Reynolds and Munn 2010).

The range depth of Barnett Shale is 1000-7500 ft. The Barnett Shale has an average temperature of 150 ºF, and is slightly over pressured with formation pressure around 3500-4400 psi and 0.52 psi/ft pressure gradient (Kanfar et al. 2013).

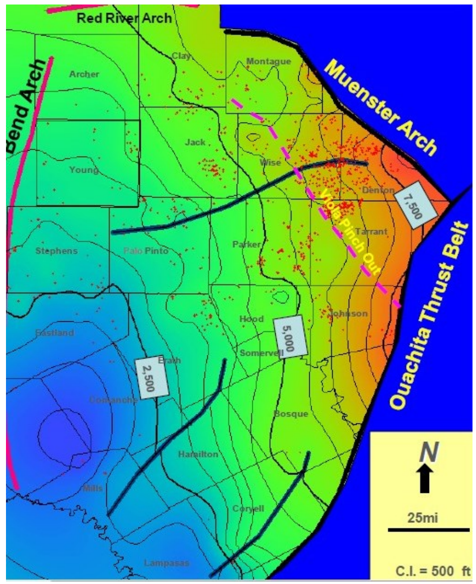

Figure 4.1: Barnett Shale Structure Map (Reynolds and Munn 2010)

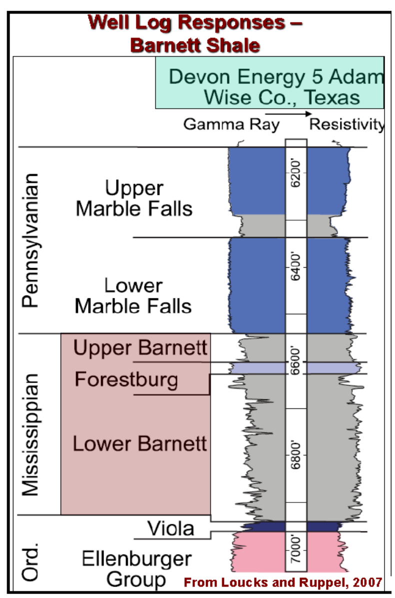

Figure 4.2: Barnett Shale Stratigraphic Map(Loucks and Ruppel,2007)

4.2 Barnett Shale Reservoir Data Overview

Data from 17 hydraulically fractured horizontal wells drilled in the Barnett Shale were analyzed in this study. The TD of those wells is around 10,300 ft. MD (7,150 ft. TVD). The average well spacing to nearby wells is 500 ft. The wells were hydraulically fractured in 3 to 15 stages with 8 to 75 perforation clusters per stage. The length of horizontal part of the wells is 2,800 ft in average. The fracture spacing range is from 50 to 500 ft. The average hydraulic fracture conductivity is less than 1 md-ft.

Production data includes daily gas and water production rate, surface casing and tubing pressure during 3.7 years production period. Figure 4.3 shows the production and pressure history of one well in Barnett Shale.

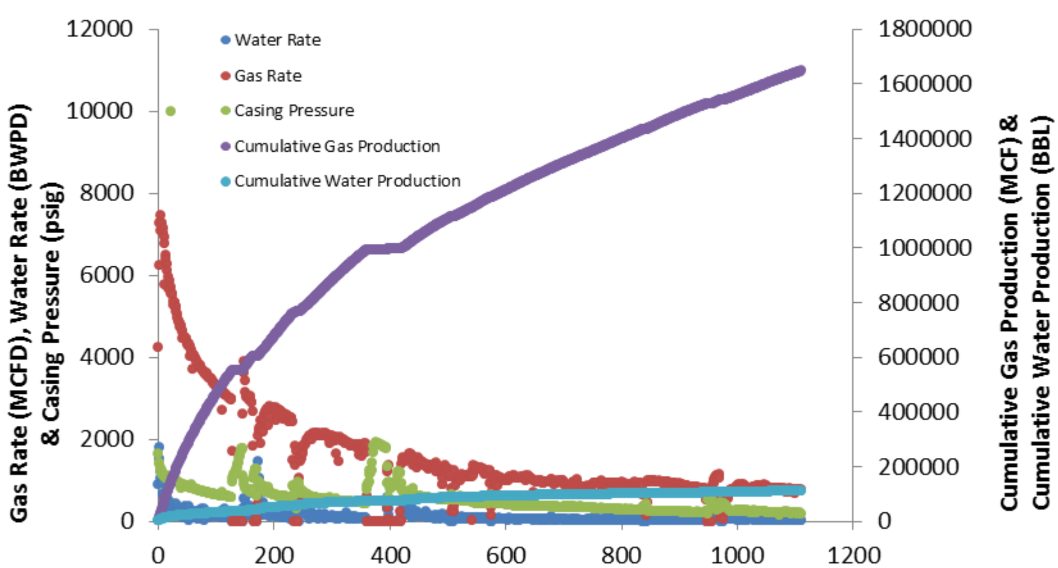

Figure 4.3: Production and Pressure History of Well in Barnett Shale

Generally water is still produced after 3 years of producing natural gas. The cumulative water does not level off during this time period. There are five shut-in periods can be recognized. After each shut-in period, gas production rates decreased and water rate increased dramatically.

4.3 Water Production Mechanism

In this section the same analysis approach as being used in Chapter III for the Horn River Shale is applied for the Barnett Shale. Diagnostic plots as well as specialized plots are used to indicate fracturing fluid flow regimes and potential production problems.

Figure 4.4 is the plot of water-gas ratio versus cumulative gas production for wells in the Barnett Shale Reservoir. We've noticed that all of these wells show a minus half slope during the early production time. However, some wells have very high water-gas ratio during the late long-term production.

Figure 4.5 shows the gas and water production as a function of time for one well in Barnett Shale. It is clear that the gas rates decreased due to some reasons, and at the same time water rates largely increased. This phenomenon was repeated two times in the production period, which causes a much higher water gas ratio in the periods of low flow rate shown in Figure 4.4.

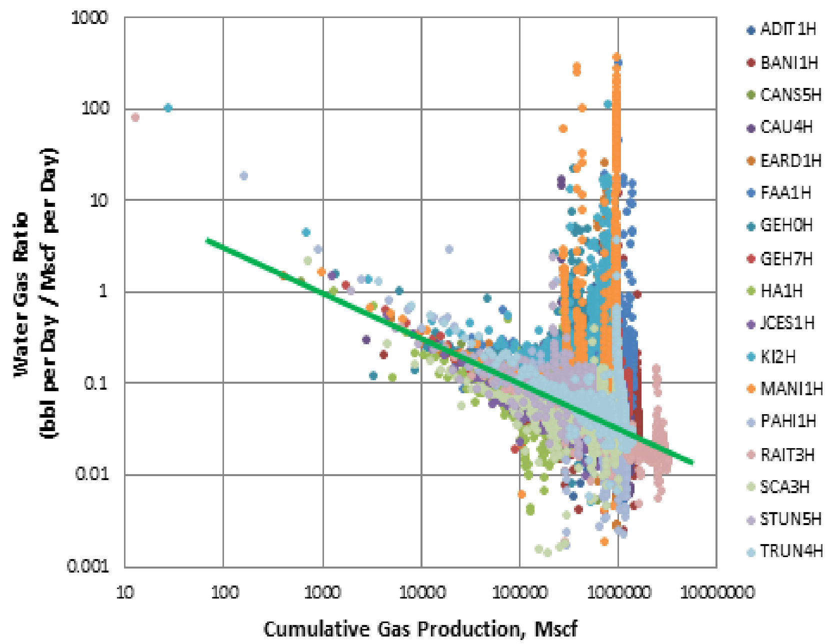

Figure 4.4 Water Gas Ratio versus Cumulative Gas Production Diagnostic Plot

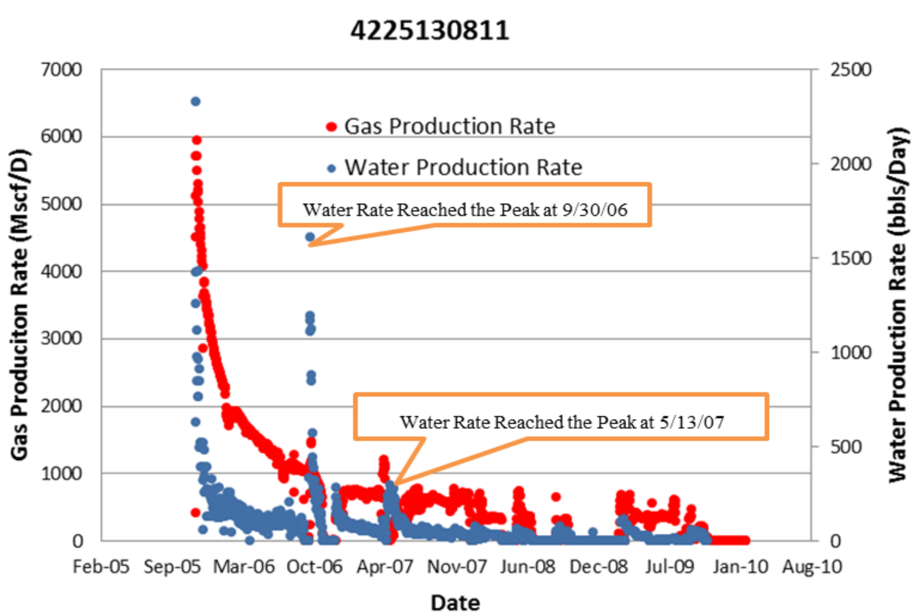

Figure 4.5 Gas and Water Production of Well 4225130811 as a Function of Time

Figure 4.6 shows the location of nearby wells which may cause the well interference for well 4225130811. We noticed that well 4225130811 was drilled closely to well 4225130503, and the shortest distance between those two wells is just 53 ft.

The shortest distance between well 4225130811 and well 4225130503 is 634 ft. The average fracture half-length of wells in Barnett Shale is 660 ft. So the well distance between those wells is short enough to cause the well interference on each other.

Table 4.1 is the summary of nearby well's information. The latest completion date of well 4225130503 was on October 1st 2006. On September 30th 2006, the water production rate of well 4225130811 reached the peak and after that started to decrease. The latest completion date of well 4225130504 was on May 14th 2007. The other water production peak rate for well 4225130811 was on May 13th 2007. This provides the evidence that the abnormally high water gas ratio during the low flow rate period may due to the well interference from nearby wells. Because right after the latest completion of nearby wells, the water production rate of well 4225130811 started to decrease.

Similar phenomenon is observed for several other wells in the Barnett Shale reservoir.

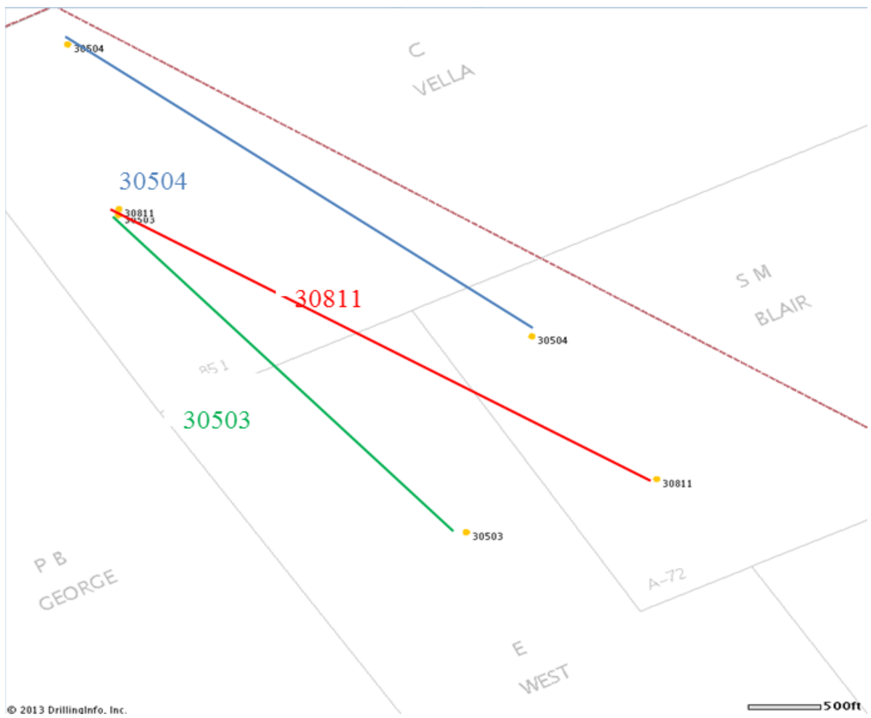

Figure 4.6 Well Location Map(Drilling Info.com)

Table 4.1: Information of Wells Possibly Causing Interference (Drilling Info.com)

API No				Liq Prod				Gas Prod			Wtr Prod
Reservoir			Basin		Comp Date	First Prod		Last Prod		Last Liq	Last Gas
	L Grav	Status	Depth	U. Perf	L. Perf	Drill Tp	TR	Sec	Latitude	Longitude	Area
42-251-30503-00				0				1203136			164132
BARNETT SHALE			FT WORTH BASIN		10/1/2006	9/1/2006		7/1/2013		0	6196
	0.0	ACTIVE	8559	9009	1[redacted]		(N/A)	0	32.5302	-97.1045	(N/A)
42-251-30504-00				1				826746			104072
BARNETT SHALE			FT WORTH BASIN		5/14/2007	5/1/2007		3/1/2013		0	1048
	0.0	INACTIVE	8487	8602	1[redacted]		(N/A)	0	32.5271	-97.0952	(N/A)

Figure 4.7 is a summary of fracturing fluid load recovery for analyzed wells in the Barnett Shale. Eight wells have load recovery more than one hundred percent. Five wells have load recovery between one hundred and one hundred fifty percent. Three well's load recovery is more than two hundred and fifty percent.

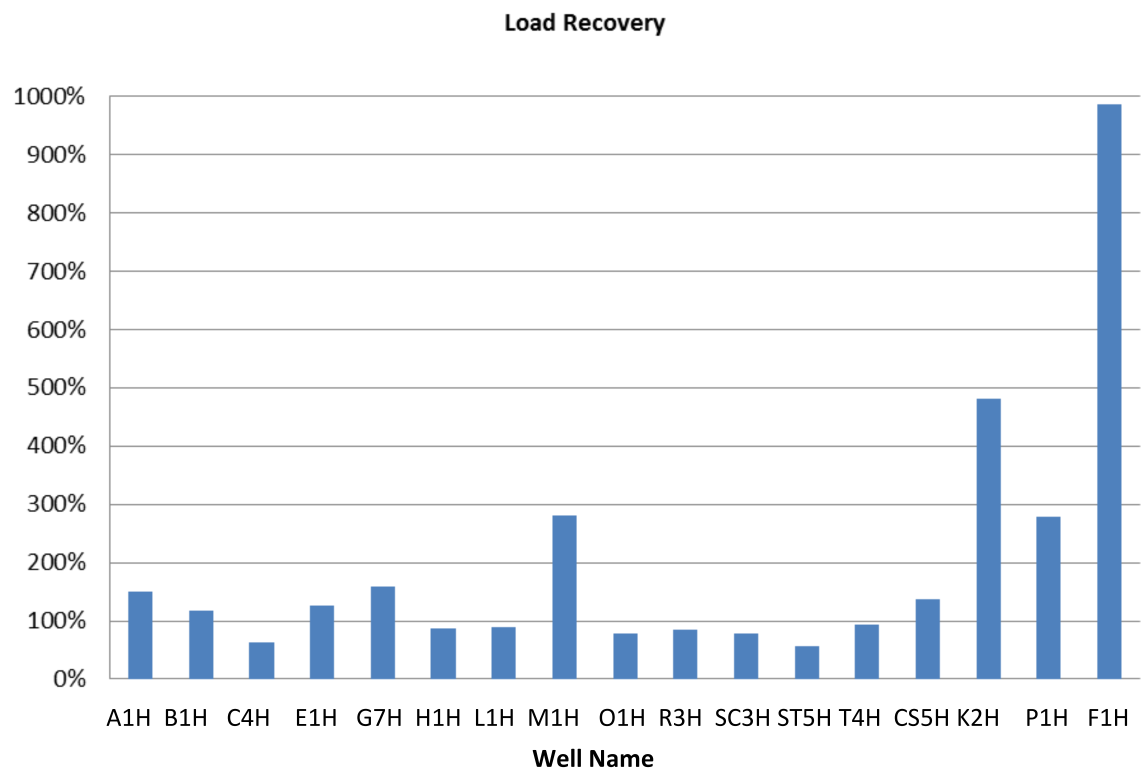

Figure 4.7: Fracturing Fluid Load Recovery of Analyzed Wells in Barnett Shale

The average true vertical depth of the analyzed wells is 7,150 ft. From Figure 4.2 we found that those wells were located in the lower Barnett Shale Unit. The reservoir unit below the lower Barnett is Ellenburger Karst, which is water bearing carbonate. Those wells with fracturing fluid load recovery higher than one hundred percent may produce water from the underlying water bearing formation Ellenburger Karst.

Figure 4.8 and Figure 4.9 show the gas production rate and water production rate for wells with significant well interference impact.

For well EARD1H, well interference results in a very high water production rate after shut-in and then water production rate drops to the same decrease trend as that before the shut-in. This is because the water production mechanism during this process is water drainage by gas, and the ability of gas lifting or carrying the water becomes smaller as the gas production rate decreases. This can be further verified by Figure 4.10 that water gas ratio of well EARD1H continues to decrease during this time. The cumulative water production for this well becomes leveling off during the long-term production period as shown in Figure 4.12.

While the water production mechanism for well FAA1H after shut-in seems different. It is shown in Figure 4.9 that the water production rate is very large after shut-in because of well interference, and then decreases to a relative constant water production rate. The water production rate continues to be in this constant range during the later production. It is very obvious that the water gas ratio gradually increases during this time as shown in Figure 4.11. In Figure 4.13, the cumulative water production still increases after five and half years' production.

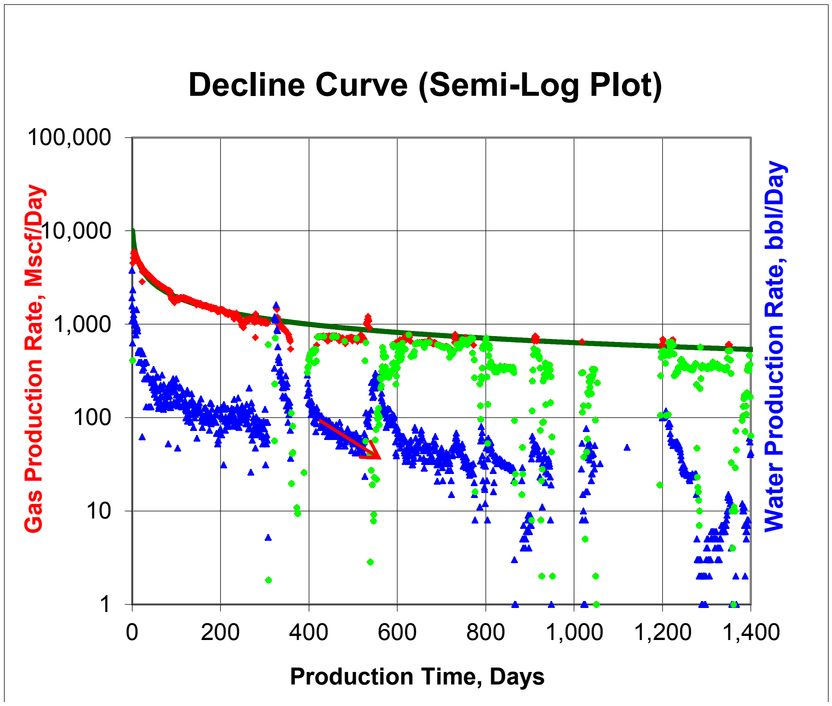

Figure 4.8: Gas Rate and Water Rate of Well EARD1H Apiwathanisorn (2013).

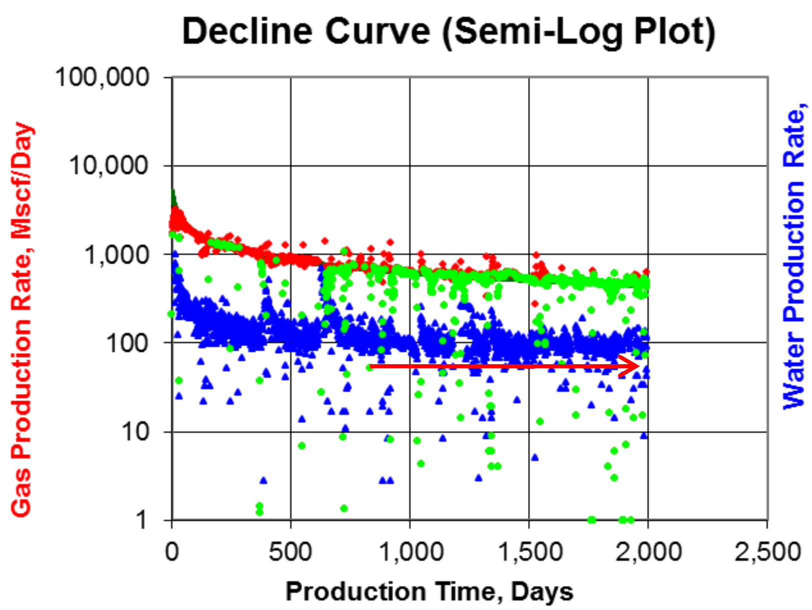

Figure 4.9: Gas Rate and Water Rate of Well FAA1H (Apiwathanisorn 2013).

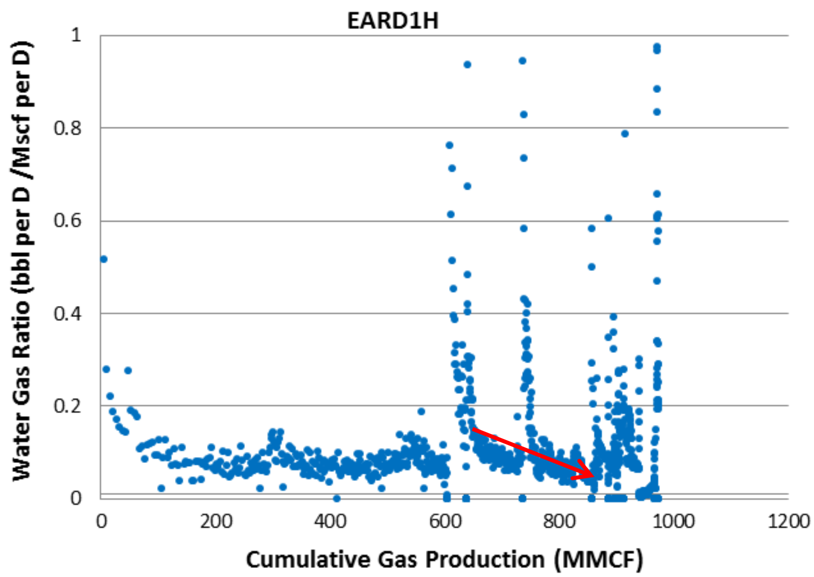

Figure 4.10: Water Gas Ratio versus Cumulative Gas of Well EARD1H

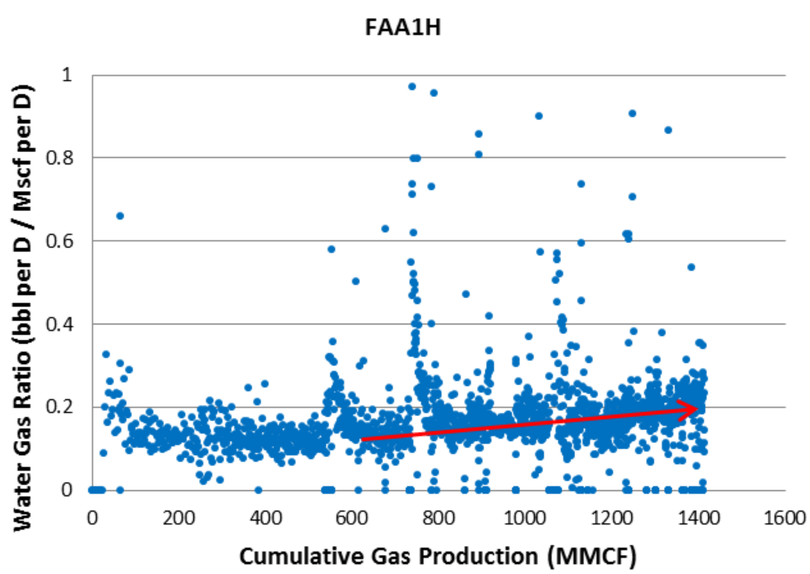

Figure 4.11: Water Gas Ratio versus Cumulative Gas of Well FAA1H

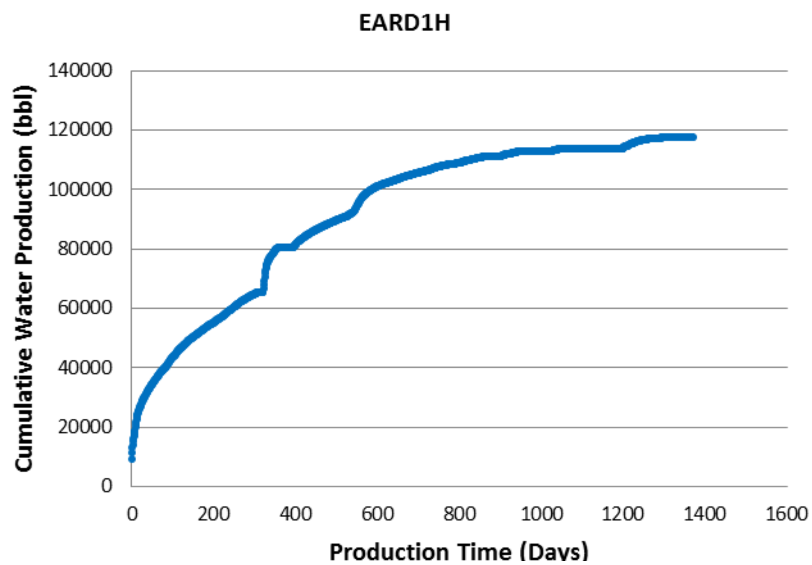

Figure 4.12: Cumulative Water Production of Well EARD1H

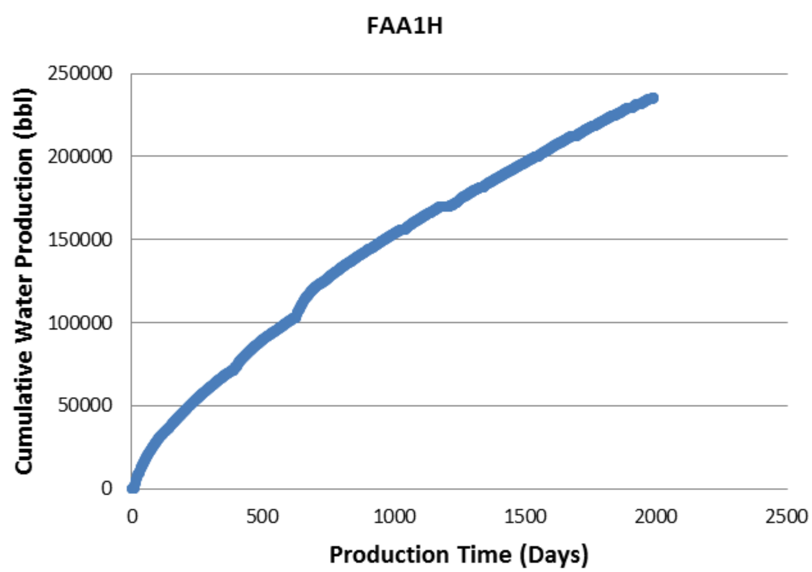

Figure 4.13: Cumulative Water Production of Well FAA1H

The analysis of fracturing fluid load recovery, water production rate, water gas ratio and cumulative water production all indicates that the well FAA1H is producing water from a formation aquifer, which probably is the underlying water bearing formation Ellenburger Karst. The water production mechanism of well FAA1H is not simply only well interference during the nearby well stimulation operation, but also producing water from another reservoir aquifer.

Water production from other source can lead to a not accurate result of fracturing fluid production analysis. We pick wells not showing the obvious character that producing water from the formation aquifer. And we select our analysis data from initial production to the time when well interference effect happens. Figure 4.14 shows the log-log plot of water gas ratio versus cumulative gas production without the biased data. The equations shown in this plot indicate that the cumulative gas and water gas ratio are statistical related. The equations also show that the trend on this plot is approach to a minus half slope. As already discussed in Chapter III, the minus half slope on log-log plot of water gas ratio versus cumulative gas means the water production mechanism is displacement regime. The water gas ratio of wells in Barnett Shale is higher than the water solubility level.

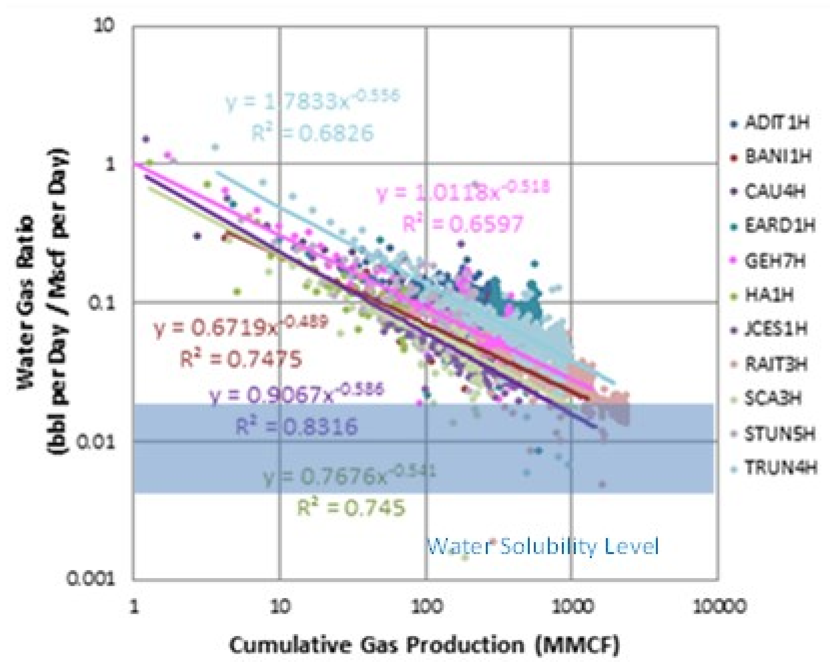

Figure 4.14: Log-Log Plot of Water Gas Ratio versus Cumulative Gas

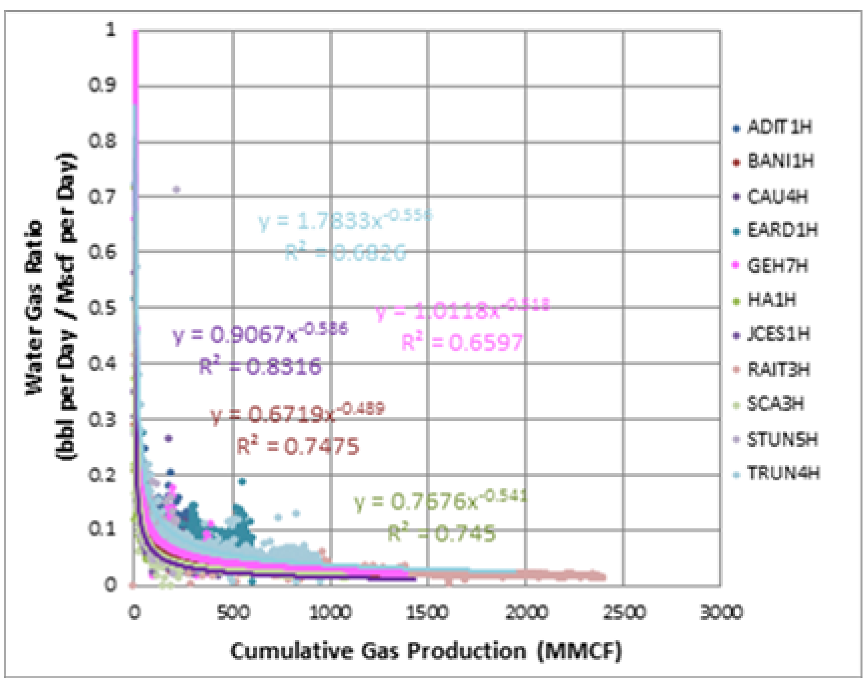

Figure 4.15: Water Gas Ratio versus Cumulative Gas Production

4.4 Analysis and Discussion of Well Performance

In this section, gas and water cumulative production and load recovery of injected fracturing fluid will be investigated to find out whether the well interference and water production from aquifer have an impact on the well production performance.

The cumulative water production versus time of the analyzed wells is shown in Figure 4.16.

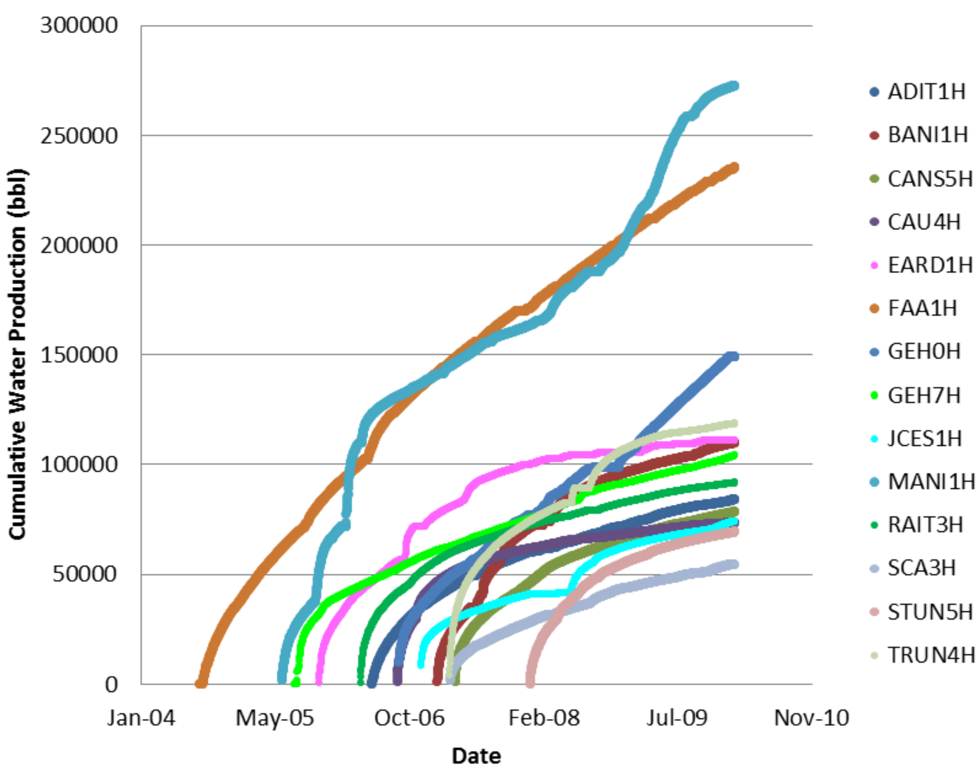

Figure 4.16: Cumulative Water Production versus Time

The cumulative water production of most of those wells becomes leveling off after more than two years' production. Well MANI1H, well FAA1H and well GEH0H have the highest cumulative water production. After more than three years' production, those three wells still have a very high water production increasing trend. Those wells may produce water from the underlying water bearing formation Ellenburger Karst.

Figure 4.17 is the cumulative gas production versus time for the analyzed wells in Barnett Shale.

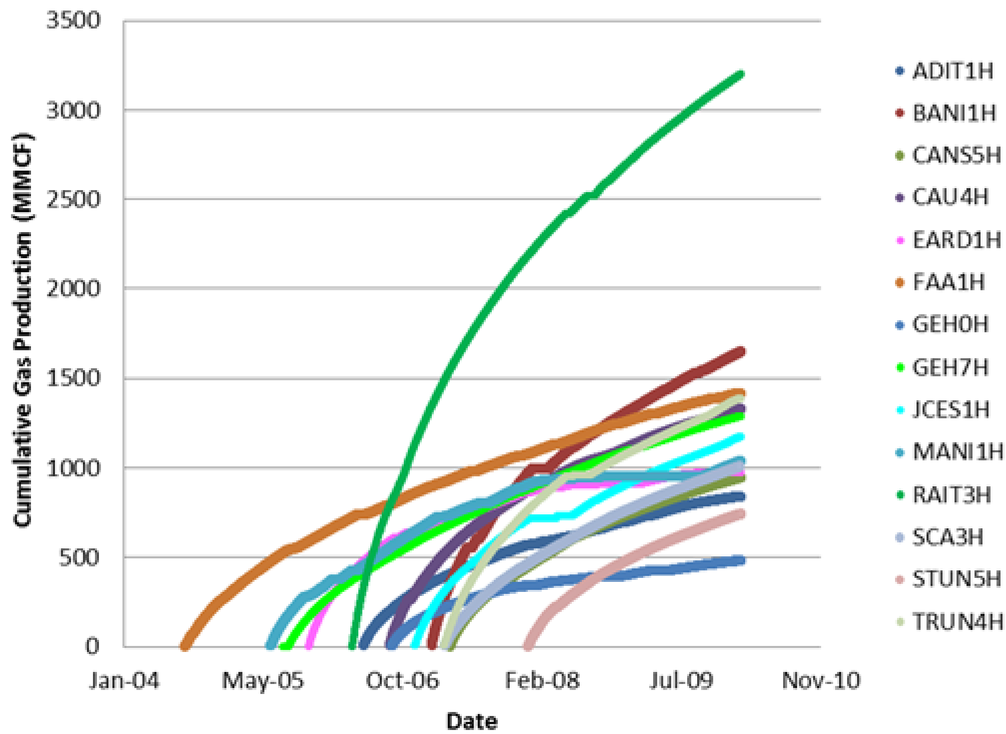

Figure 4.17: Cumulative Gas Production versus Time

Basically the gas production increase trend of most wells is very similar. Because of producing water from formation aquifer, well MANI1H stopped producing natural gas for more than one year. Well GEH0H has the lowest cumulative gas production probably because it also produces water from the underlying aquifer.

We selected the data from initial production until the time when well interference happened for wells not producing water from formation aquifer. Figure 4.18 is the load recovery versus cumulative gas production plot. As for Horn River, we observe load recoveries that are much larger than the typical 25% or less reported by many operators. However, despite the observed very high load recovery values in some wells, the displacement regime dominates water flowback behavior from the Barnett shale wells, suggesting that the ultimate load recovery could be even higher. None of the wells in Figure 4.18 show evidence that the high water production is linked to flow from the adjacent Ellenberger aquifer.

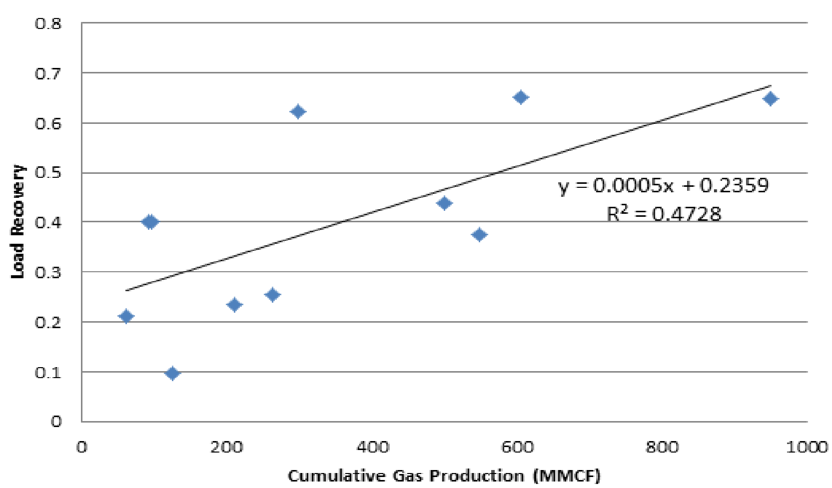

Figure 4.18: Load Recovery versus Cumulative Gas Production

4.5 Chapter IV Summary

In this chapter, the water production behavior of the Barnett shale has been investigated using log-log diagnostic and some analysis plots. The displacement regime dominates water flowback behavior from the Barnett Shale wells. This is because the shear dominated complexity may be water filled in Barnett Shale. The higher water gas ratio departure from the minus half slope trend shows that well interference happens in some wells. Some wells may produce water from the underlying aquifer formation, and this has negative impact on well performance.

CHAPTER V

CONCLUSIONS AND RECOMMENDATIONS

This chapter includes the summary of our research work, our conclusions from the study, and recommendations on future work.

5.1 Conclusions

The main objective of this study is to determine the fracturing fluid production mechanisms of hydraulically fractured horizontal wells in different shale gas reservoirs and find out any potential production problems linked to the ultimate load recovery.

The log-log plot of water gas ratio versus cumulative gas production seems to identify drainage and vaporization fracturing fluid production mechanisms for 15 wells in Horn River Shale reservoir and 17 wells in Barnett Shale reservoir. This empirical plot shows apparent straight trends, first -1/2 and then -1. For Horn River Shale, the diagnostic plot shows a nearly minus half slope followed by a slope approaching minus one. In Barnett Shale, only the nearly minus half slope is shown in the log-log plot of water gas ratio versus cumulative gas production.

Furthermore, we used the pressure and temperature data to estimate the water solubility level in Horn River Shale gas reservoir and Barnett Shale gas reservoir. When the range in the solubility level is compared to the observed WGR behavior, it appears that the -1/2 slope behavior may represent drainage, and the -1 slope behavior may represent vaporization.

In Horn River Shale, during the -1/2 slope trend on the log-log graph of WGR versus cumulative gas production, the WGR is well above the solubility level, and the wells approach WGR consistent with water solubility in late time while -1 slope trend dominates. The vaporization behavior occurs while the load recovery is less than one. If the WGR drops below water solubility indicating undersaturated gas, and load recovery is still less than one, this may be a sign that water blocks gas flow in part of the reservoir.

In Barnett Shale, while only the -1/2 slope behavior is observed on the graph of WGR versus cumulative gas production, the water gas ratio remains higher than the water solubility level. Both of these observations suggest that the wells are still in the drainage regime and that the load recovery will continue to increase. It is also interesting to note that the load recoveries in both Horn River and Barnett wells are considerably higher than typical 15-25% load recoveries reported by many shale gas operators. Water produced during drainage impacts well performance, while water produced by vaporization does not.

The log-log diagnostic plot can also indicate potential production problems. Large upward departures from these trends seem to indicate well interference or water production from an aquifer. These phenomena are observed in several Barnett Shale wells. Large downward departures from the -1 trend are consistent with liquid loading in one Horn River well.

Well interference is often linked to hydraulic fracturing in nearby wells. It may be observed as increased water production and decreased gas production after wells were shut in during the neighboring well stimulation work. During fracturing the hydraulic fracturing fluid flows into the wells that have been on production through existing and actively created hydraulic fractures because the pressure in produced wells is much lower. Well interference represents intersecting hydraulic or secondary fractures, and this could be an indication that wells could be spaced further apart. When wells are put on production at the same time, absence of such anomalies is not an indication that the fractures do not intersect. The nature of observed interference behavior is different when it is related to adjacent pad development.

5.2 Recommendations for Future Work

Based on this research work, we recommend for the future work to consider the produced water chemistry. This could entail deliberate use of tracers or simply contrasting between injected fracturing fluid and water from an adjacent formation. This would help to understand the origin of produced water and provide additional insight on the water production mechanisms. Further, it would be useful to analyze data from other shale formations to see whether the trends observed for Horn River and Barnett shale formations are repeated. If they are, it would be especially useful to develop a physical generalization for the drainage and vaporization trends.

REFERENCES

Agnia, A., Alkouh, A.B., and Wattenbarger, R. 2012. Bias in Rate-Transient Analysis Methods: Shale Gas Wells. Paper SPE-159710-MS presented at the SPE Annual Technical Conference and Exhibition, San Antonio, Texas, USA. 8-10 October 2012. Society of Petroleum Engineers.

Apiwathanasorn, S. 2013. Evidence of Reopened Microfractures in Production Data of Hydraulically Fractured Shale Gas Wells.

Batohie, G. and Maharaj, G. 2012. Frac-Packing Shallow Unconsolidated Reservoirs - Onshore Trinidad. Paper SPE-158214-MS presented at the SPETT 2012 Energy Conference and Exhibition, Port-of-Spain, Trinidad. 11-13 June 2012. Society of Petroleum Engineers.

Cheng, Y. 2010. Impact of Water Dynamics in Fractures on the Performance of Hydraulically Fractured Wells in Gas Shale Reservoirs. Paper SPE-127863-MS presented at the SPE International Symposium and Exhibiton on Formation Damage Control, Lafayette, Louisiana, USA. 10-12 February 2010. Society of Petroleum Engineers.

Clarkson, C.R. 2012. Modeling 2-Phase Flowback of Multi-Fractured Horizontal Wells Completed in Shale. Paper SPE-162593-MS presented at the SPE Canadian Unconventional Resources Conference, Calgary, Alberta, Canada. 30 October-1 November 2012. Society of Petroleum Engineers.

Crafton, J.W. 2010. Flowback Performance in Intensely Naturally Fractured Shale Gas Reservoirs. Paper SPE-131785-MS presented at the SPE Unconventional Gas Conference, Pittsburgh, Pennsylvania, USA. 23-25 February 2010. Society of Petroleum Engineers.

Crafton, J.W. and Gunderson, D.W. 2006. Use of Extremely High Time-Resolution Production Data to Characterize Hydraulic Fracture Properties. Paper SPE-103591-MS presented at the SPE Annual Technical Conference and Exhibition, San Antonio, Texas, USA. 24-27 September 2006. Society of Petroleum Engineers.

Ehlig-Economides, C.A., Ahmed, I.A., Apiwathanasorn, S., Lightner, J.H., Song, B., Rosales, F.E.V., Xue, H., and Zhang, Y. 2012. Stimulated Shale Volume Characterization: Multiwell Case Study from the Horn River Shale: Ii. Flow Perspective. Paper SPE-159546-MS presented at the SPE Annual Technical Conference and Exhibition, San Antonio, Texas, USA. 8-10 October 2012. Society of Petroleum Engineers.

Holditch, S.A. 1979. Factors Affecting Water Blocking and Gas Flow from Hydraulically Fractured Gas Wells. *Journal of Petroleum Technology* **31** (12): 1515-1524. 00007561

Ilk, D., Currie, S.M., Symmons, D., Rushing, J.A., Broussard, N.J., and Blasingame, T.A. 2010. A Comprehensive Workflow for Early Analysis and Interpretation of Flowback Data from Wells in Tight Gas/Shale Reservoir Systems. Paper SPE-135607-MS presented at the SPE Annual Technical Conference and Exhibition, Florence, Italy. 19-22 September 2010. Society of Petroleum Engineers.

Johnson, M.F., Walsh, W., Budgell, P.A., and Davidson, J.A. 2011. The Ultimate Potential for Unconventional Gas in the Horn River Basin: Integrating Geological Mapping with Monte Carlo Simulations. Paper SPE-148976-MS presented at the Canadian Unconventional Resources Conference, Alberta, Canada. 15-17 November 2011. Her Majesty the Queen in Right of Canada 2011.

Kanfar, M., Alkouh, A., and Wattenbarger, R. 2013. Modeling Guidelines for Analyzing and Forecasting Shale Well Performance. Paper SPE-165698-MS presented at the 2013 SPE Eastern Regional Meeting, Pittsburgh, Pennsylvania, USA. Aug 20 - 22 2013. 2013, Society of Petroleum Engineers.

King, G.E. 2010. Thirty Years of Gas Shale Fracturing: What Have We Learned? Paper SPE-133456-MS presented at the SPE Annual Technical Conference and Exhibition, Florence, Italy. 19-22 September 2010. Society of Petroleum Engineers.

Kuru, E., Parmar, J., and Dehghanpour, H. 2013. Drainage against Gravity: Factors Impacting the Load Recovery in Fractures. Paper SPE-164530-MS presented at the SPE Unconventional Resources Conference - USA, The Woodlands, TX, USA. Apr 10 - 12, 2013 2013. 2013, Society of Petroleum Engineers.

Leonard, R.S., Woodroof, R.A., Bullard, K., Middlebrook, M.L., and Wilson, R.E. 2007. Barnett Shale Completions: A Method for Assessing New Completion Strategies. Paper SPE-110809-MS presented at the SPE Annual Technical Conference and Exhibition, Anaheim, California, U.S.A. 11-14 November 2007. Society of Petroleum Engineers.

Lolon, E., Mayerhofer, M.J., Garcia, I., Durey, D.A., Byrd, A.C., and Rhodes, R.D. 2008. Integrated Fracture and Production Modeling Study in the Lower Cotton Valley Sands, Northern Louisiana. Paper SPE-115467-MS presented at the SPE Annual Technical Conference and Exhibition, Denver, Colorado, USA. 21-24 September 2008. Society of Petroleum Engineers.

Mahadevan, J., Yortsos, Y.C., and Sharma, M.M. 2005. Evaporative Clean-up of Water-Blocks in Gas Wells. Paper SPE-94215-MS presented at the SPE Production Operations Symposium, Oklahoma City, Oklahoma. 16-19 April 2005. Society of Petroleum Engineers.

Maxwell, S.C., Shemeta, J.E., Campbell, E., and Quirk, D.J. 2008. Microseismic Deformation Rate Monitoring. Paper SPE-116596-MS presented at the SPE Annual Technical Conference and Exhibition, Denver, Colorado, USA. 21-24 September 2008. Society of Petroleum Engineers.

Modeland, N., Buller, D., and Chong, K.K. 2011. Statistical Analysis of Completion Methodology's Effect on Production in the Haynesville Shale. Paper SPE-144120-MS presented at the North American Unconventional Gas Conference and Exhibition, The Woodlands, Texas, USA. 14-16 June 2011. Society of Petroleum Engineers.

Munoz, A.V., Asadi, M., Woodroof, R.A., and Morales, R. 2009. Long-Term Post-Frac Performance Analysis Based on Flowback Analysis Using Chemical Frac-Tracers. Paper SPE-121380-MS presented at the Latin American and Caribbean Petroleum Engineering Conference, Cartagena de Indias, Colombia. 31 May-3 June 2009. Society of Petroleum Engineers.

Newsham, K.E., Rushing, J.A., and Lasswell, P.M. 2003. Use of Vapor Desorption Data to Characterize High Capillary Pressures in a Basin-Centered Gas Accumulation with Ultra-Low Connate Water Saturations. Paper 00084596 presented at the SPE Annual Technical Conference and Exhibition, Denver, Colorado. 5-8 October 2003. Society of Petroleum Engineers.

Parekh, B. and Sharma, M.M. 2004. Cleanup of Water Blocks in Depleted Low-Permeability Reservoirs. Paper 00089837 presented at the SPE Annual Technical Conference and Exhibition, Houston, Texas. 26-29 September 2004. Society of Petroleum Engineers.

Reynolds, M.M. and Munn, D.L. 2010. Development Update for an Emerging Shale Gas Giant Field - Horn River Basin, British Columbia, Canada. Paper SPE-130103-MS presented at the SPE Unconventional Gas Conference, Pittsburgh, Pennsylvania, USA. 23-25 February 2010. Society of Petroleum Engineers.

Rushing, J.A., Newsham, K.E., Fraassen, K.C.V., Mehta, S.A., and Moore, G.R. 2008. The Catalytic Effects of Nonhydrocarbon Contaminants on Equilibrium Water Vapor Content for a Dry Gas at Hp/Ht Reservoir Conditions. Paper SPE-114517-MS presented at the CIPC/SPE Gas Technology Symposium 2008 Joint Conference, Calgary, Alberta, Canada. 16-19 June 2008. Society of Petroleum Engineers.

Sage, B.H. and Lacey, W.N. 1955. *Some Properties of the Lighter Hydrocarbons, Hydrogen Sulfide, and Carbon Dioxide: Monograph on Api Research Project 37*: American Petroleum Institute.

Thompson, J.W., Fan, L., Grant, D., Martin, R.B., Kanneganti, K.T., and Lindsay, G.J. 2010. An Overview of Horizontal Well Completions in the Haynesville Shale. Paper SPE-136875-MS presented at the Canadian Unconventional Resources and International Petroleum Conference, Calgary, Alberta, Canada. 19-21 October 2010. Society of Petroleum Engineers.

Turner, R.G., Hubbard, M.G., and Dukler, A.E. 1969. *Analysis and Prediction of Minimum Flow Rate for the Continuous Removal of Liquids from Gas Wells*.

Warpinski, N.R., Mayerhofer, M.J., Vincent, M.C., Cipolla, C.L., and Lolon, E. 2008. Stimulating Unconventional Reservoirs: Maximizing Network Growth While Optimizing Fracture Conductivity. Paper SPE-114173-MS presented at the SPE Unconventional Reservoirs Conference, Keystone, Colorado, USA. 10-12 February 2008. Society of Petroleum Engineers.

Whitson, C.H., Rahmawati, S.D., and Juell, A. 2012. Cyclic Shut-in Eliminates Liquid-Loading in Gas Wells. Paper SPE-153073-MS presented at the SPE/EAGE European Unconventional Resources Conference and Exhibition, Vienna, Austria. 20-22 March 2012. Society of Petroleum Engineers.

Willberg, D.M., Steinsberger, N., Hoover, R., Card, R.J., and Queen, J. 1998. Optimization of Fracture Cleanup Using Flowback Analysis. Paper 00039920 presented at the SPE Rocky Mountain Regional/Low-Permeability Reservoirs Symposium, Denver, Colorado. 5-8 April 1998. Copyright 1998, Society of Petroleum Engineers Inc.

Zhou, D. and Yuan, H. 2009. New Model for Gas Well Loading Prediction. Paper SPE-120580-MS presented at the SPE Production and Operations Symposium, Oklahoma City, Oklahoma. 4-8 April 2009. Society of Petroleum Engineers.